2011

MICE LACKING MIST1 SHOW INCREASED SENSITIVITY TO CHRONIC ETHANOL EXPOSURE

Sruthi Alahari

MICE LACKING MIST1 SHOW INCREASED SENSITIVITY TO CHRONIC ETHANOL EXPOSURE

MIST1 AND CHRONIC ETHANOL EXPOSURE

(Thesis Format: Monograph)

by

Sruthi Alahari

Graduate Program in Physiology and Pharmacology

A thesis submitted in partial fulfillment of the requirements for the degree of Master of Science

The School of Graduate and Postdoctoral Studies

The University of Western Ontario

London, Ontario, Canada

THE UNIVERSITY OF WESTERN ONTARIO
SCHOOL OF GRADUATE AND POSTDOCTORAL STUDIES

CERTIFICATE OF EXAMINATION

Supervisor

Dr. Christopher Pin

Supervisory Committee

Dr. Barry Tepperman

Dr. Peter Chidiac

Examiners

Dr. Lina Dagnino

Dr. Sean Cregan

Dr. Murray Huff

The thesis by

Sruthi Alahari

entitled:

Mice lacking MIST1 show increased sensitivity to chronic ethanol exposure

is accepted in partial fulfilment of the
requirements for the degree of

Master of Science

Date October 27, 2011

Dr. Cheryle Seguin (Chair of the thesis examining board)

Abstract

Rodent models show that alcohol only sensitizes the pancreas to subsequent insult, indicating that additional factors play a role in alcohol-induced pancreatic injury. Mice lacking MIST1 (*Mist1*$^{-/-}$), a target of the UPR marker XBP1, show reduced ability to activate the UPR during cell stress. Therefore, I hypothesized that an absence of MIST1 would lead to increased sensitivity to alcohol feeding. The effects of dietary stress on the UPR were examined in pancreatic tissue from 2 to 4 month-old mice placed on a diet containing 36% of kcal from ethanol for 6 weeks. Based on immunofluorescent, histological and immunoblotting assays, *Mist1*$^{-/-}$ mice showed age related changes in UPR activation. In response to ethanol, they developed periductal accumulations of inflammatory cells, limited induction of autophagy and reduction in the expression of BiP, peIF2α and *sXbp1*, unlike wild type counterparts that had significantly higher levels of *sXbp1* and peIF2α. The UPR was not further activated following initiation of acute pancreatitis. This work suggests that factors affecting MIST1 expression and function in humans may be a predisposing factor for pancreatic disease.

Keywords: Pancreas, MIST1, Unfolded Protein Response, Ethanol diet, High-fat diet, Autophagy

ACKNOWLEDGEMENTS

I would like to thank my supervisor, Dr. Christopher Pin for his continued support, encouragement and advice throughout this project. He has set high standards for our lab and always pushed me to do my best. In addition to being a vast source of knowledge, his accessibility and friendly nature have made the journey that much smoother.

I would also like to acknowledge members of the Pin lab, Charis Johnson, Elena Fazio, Dr. Rashid Mehmood and Camilla Stepniak for all their help, academic and otherwise. It was a pleasure to work in such a wonderful, friendly environment. Their continued encouragement and positive critiques have helped shape my work. Thank you to the Deroo, Drysdale and DiMattia-Shepherd labs for their ideas and comments during group lab meetings. Members of my advisory committee, Drs. Barry Tepperman and Peter Chidiac have been most helpful in offering suggestions and valuable feedback all the way. Last but not the least, I would like to thank my family for their unending love and support and for picking me up when I was down.

TABLE OF CONTENTS

LIST OF FIGURES AND TABLES

TABLE **PAGE**

ABBREVIATIONS

ACh	Acetylcholine
ANOVA	Analysis of variance
ASK1	Apoptosis signal-regulating kinase 1
Atg	Autophagy related gene
ATP	Adenosine triphosphate
ATF3	Activating transcription factor 3
ATF4	Activating transcription factor 4
ATF6	Activating transcription factor 6
bHLH	Basic helix-loop-helix
bZIP	Basic leucine zipper
cAMP	Cyclic adenosine monophosphate
CRE	Cyclic adenosine monophosphate response element
CHOP	CCAAT/enhancer binding protein homologous protein
CE	Cholesteryl ester
CPA	Carboxypeptidase
CCK	Cholecystokinin
CTRC	Chymotrypsinogen C
CYP2E1	Cytochrome P 450 2E1
DAG	Diacylglycerol
DAPI	4,6 diamidino-2-phenylindole
DEPC	Diethyl pyrocarbonate
DNA	Deoxyribose nucleic acid
dNTP	deoxy-nucleotide triphosphate

eIF2α	Eukaryotic initiation factor 2 α
ER	Endoplasmic reticulum
ERSE-1	Endoplasmic reticulum stress response element 1
FAEE	Fatty acid ethyl ester
FITC	Fluorescein iso-thiocyanate
GADD34	Growth arrest and DNA damage inducible protein 34
GDP	Guanine diphosphate
GPCR	G protein coupled receptor
GTP	Guanine triphosphate
HRP	Horse radish peroxidase
IF	Immunofluorescence
IP_3	Inositol 1,4,5-triphosphate
IP_3R	Inositol 1,4,5-triphosphate receptor
IRE1	Inositol requiring enzyme 1
kDa	Kilodalton
kcal	Kilocalories
LPL	Lipoprotein lipase
MIST1	Muscle, inhibitor of Twist-1
NFDM	Non-fat dried milk
NF-κB	Nuclear factor –kappa B
PAGE	Polyacrylamide gel electrophoresis
PAP1	Pancreatitis associated protein 1
PAR	Protease activated receptor
PBS	Phosphate buffered saline
PBS-T	Phosphate buffered saline with Tween-20

PCR	Polymerase chain reaction
PRSS1	Protease, Serine 1
PSP	Pancreatic stone protein
peIF2α	Phosphorylated eukaryotic initiation factor 2 α
PERK	*Protein* kinase RNA (PKR)-like endoplasmic reticulum kinase
pPERK	Phosphorylated *PERK*
PLC	Phospholipase C
PVDF	Polyvinylidene difluoride
RNA	Ribose nucleic acid
RT	Reverse transcription
RT-PCR	Reverse transcription polymerase chain reaction
SDS	Sodium dodecyl sulfate
SNARE	Soluble N-ethylmaleimide-sensitive fusion protein attachment protein receptors
SPINK1	Serine protease inhibitor Kazal type 1
TBS	Tris buffered saline
TBS-T	Tris buffered saline with Tween-20
TRAF2	Tumour necrosis factor receptor associated factor 2
TRITC	Tetramethylrhodamine isothiocyanate
uORF	Upstream open reading frame
UPR	Unfolded protein response
UPRE	Unfolded protein response element
UTR	Untranslated region
VAMP	Vesicle associated membrane protein
WT	Wild type

XBP1/*Xbp1*	X-box binding protein 1
sXBP1/Xbp1	Spliced XBP1/*Xbp1*
uXBP1/Xbp1	Unspliced XBP1/*Xbp1*
ZG	Zymogen granule

CHAPTER 1: INTRODUCTION

The pancreas is a glandular organ that is the main site of digestive enzyme synthesis in the body. The pancreas consists of exocrine, endocrine and ductal cell compartments that are distinct in morphology and function. The endocrine compartment comprises 2% of total pancreatic area in the rat and is confined to the islets of Langerhans (Kempen, de Pont & Bonting, 1977). The endocrine pancreas is responsible for the secretion of the glucose-regulating hormones insulin and glucagon, as well as somatostatin, pancreatic polypeptide and ghrelin (Elayat, el-Naggar & Tahir, 1995. The cell types that secrete these hormones are as follows: alpha cells produce glucagon; beta cells produce insulin and amylin; delta cells produce somatostatin; pancreatic polypeptide cells produce pancreatic polypeptide and epsilon cells produce the hormone ghrelin (Elayat, el-Naggar & Tahir, 1995). Pancreatic duct cells play an integral role in the exocrine function of the organ by producing bicarbonate and mucin rich secretions required for digestion and providing a passageway for digestive enzymes to the duodenum of the small intestine (Kuijpers & de Pont, 1987). The focus of this thesis is on the exocrine pancreas and its response to environmental stressors.

1.1 THE ACINAR CELL

The functional unit of the exocrine pancreas is the acinus, which is comprised of acinar cells (**Figure 1.1**). Acinar cells are designed for the synthesis, storage and secretion of digestive enzymes into pancreatic ducts. Hence, the acinar cell contains an extensive endoplasmic reticulum (ER) and Golgi apparatus to cope with the high rate of

protein synthesis (Hand, 1990). Morphologically, acinar cells are pyramidal in shape and characterized by apical-basal polarity of intracellular organelles (McCuskey & Chapman, 1969). While the nucleus and endoplasmic reticulum (ER) are basally localized, secretory vesicles known as zymogen granules are predominantly concentrated at the apex (McCuskey & Chapman, 1969). Secretory proteins pass from the rough endoplasmic reticulum (ER) to the Golgi apparatus where they are concentrated into condensing vacuoles as zymogens (Hand, 1990). A pancreatic zymogen is an inactive precursor or proenzyme that is activated in the duodenum by cleavage of the peptide bond in its amino-terminal region (Rinderknecht et al, 1974). In the presence of low concentrations of Ca^{2+} in the duodenum, the enzyme enteropeptidase (enterokinase) cleaves the terminal hexapeptide from inactive trypsinogen to form active trypsin. This first crucial cleavage reaction subsequently triggers the activation of all other pancreatic zymogens (Rinderknecht et al, 1974), which include chymotrypsinogen proelastase, procarboxypeptidase and prophospholipase A. Enzymes secreted in their active form include amylase, lipase, cholesterol esterase, ribonuclease and deoxyribonuclease, colipase and pancreatic trypsin inhibitor (reviewed by Case, 1978).

Figure 1.1. Structure of a pancreatic acinar cell. The acinar cell exhibits apical-basal polarity with the nucleus and endoplasmic reticulum localized to the basal aspect (facing the basement membrane) and zymogen granules (storage vesicles) containing digestive enzyme precursors localized to the apical pole. Through the process of regulated exocytosis, the contents of the zymogen granules are released into the acinar lumen, which is continuous with pancreatic ducts.

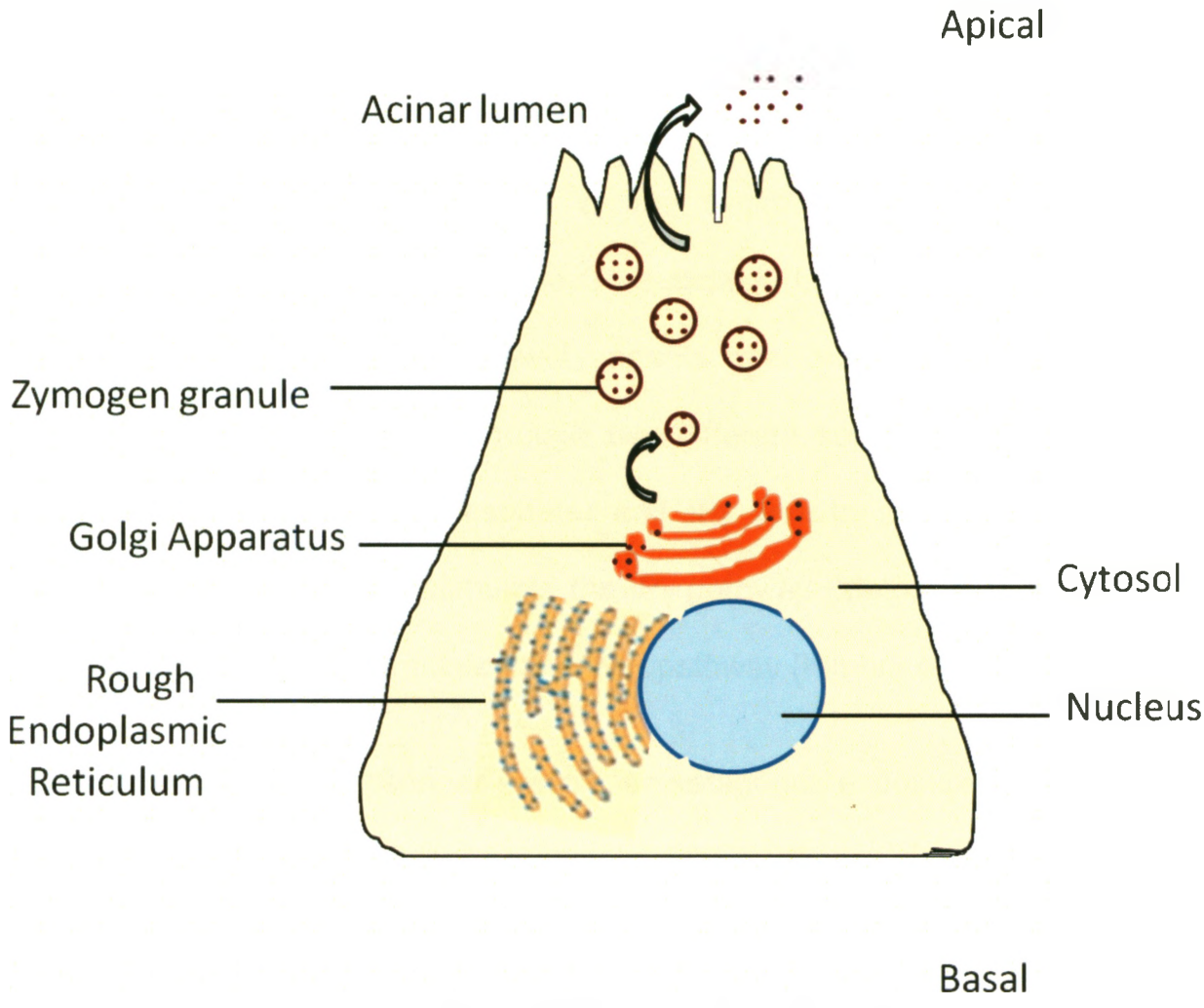

Adapted from Lodish et al, 2000.

Pancreatic enzyme secretion is predominantly regulated via a hormonal pathway mediated by gastrointestinal hormones such as cholecystokinin (CCK) and a cholinergic pathway mediated by the neurotransmitters such as acetylcholine (ACh) (Owyang, 1996). In addition to the binding and activation of high affinity CCKA receptors on pancreatic vagal afferents, rodent and human acinar cells have functional CCK receptors on the basolateral plasma membrane that, upon stimulation, can initiate a signalling cascade that regulates exocytosis (Owyang, 1996; Murphy et al, 2008). These receptors belong to members of the G-protein coupled receptor family, specifically heterotrimeric proteins of the Gq subclass (Logsdon, 1994; Yule, Baker & Williams, 1999). At the cellular level, agents that stimulate secretion, termed secretagogues initiate exocytosis through two different second messenger systems: cAMP (cyclic adenosine monophosphate) and IP_3 (inositol triphosphate). While the secretagogues, CCK and ACh stimulate the IP_3 pathway (Matozaki et al, 1990), other hormones such as secretin stimulate the cAMP pathway (Kimura et al, 1986).

In the IP_3 second messenger system, secretagogue exposure induces activation of the α subunit of the Gq family of receptors, which triggers phospholipase C and in turn stimulates the production of inositol-3-phosphate (IP_3) and diacylglycerol (DAG). IP_3 regulates Ca^{2+} release from intracellular reserves while DAG activates protein kinase C (PKC) (Matozaki, 1990; Yule, Baker & Williams, 1999). Under non-stress conditions, secretagogue stimulation of pancreatic acinar cells leads to an oscillatory rise in intracellular Ca^{2+} levels, followed by spreading of the signal (Thorn et al, 1993; reviewed by Logsdon, 2000). This signal subsequently leads to the fusion of zymogen granule membranes to the apical plasma membrane of the acinar cell, believed to be mediated

by the proteins, soluble NSF attachment protein receptor (SNARE) and Rab (belonging to the Ras superfamily of monomeric G-proteins)(Sudhof, 1995). Following fusion, contents of the zymogen granules are released into the ductal system for transport to the duodenum.

Under non-physiological conditions, such as those following hyperstimulation of the CCK receptors to induce mild acute pancreatitis, the secretagogue induced exocytosis pathway is disrupted. According to one hypothesis, major events include the co-localization of zymogens and lysosomal enzymes such as cathepsin B into large vacuoles. It is believed that premature trypsinogen cleavage and activation occurs in these compartments where the pH is acidic and favours enzyme activation (Willemer et al, 1990; Steer & Meldolesi, 1988). Rise in intracellular Ca^{2+} levels aids the formation of these cytosolic vacuoles (Kruger et al, 2000; Raraty et al, 2000). Additionally, the process of exocytosis is said to be redirected from the apical pole to the basolateral aspects of the cell, resulting in elevated levels of digestive enzymes in the pancreatic interstitium (Scheele et al, 1987).

The acinar cell has evolved three major defense mechanisms to protect itself from autodigestive injury in the event of premature intracellular enzyme activation. A key feature of pancreatic digestive enzymes is that most of them are synthesized, packaged and secreted in their inactive, precursor form (termed zymogen). These zymogens are often proteases that are designed to be activated only upon arrival at the duodenum where they aid in digestion in a pH dependent manner. Second, restriction of both inactive and active enzymes (such as amylase, which is not produced as a precursor) to zymogen granules prevents unwanted contact with other intracellular organelles,

thereby preserving cellular integrity. Third, genetic mechanisms that either inhibit further activation of, or degrade active intracellular proteases are in place. Serine protease inhibitor kazal type 1 (SPINK1) encodes an endogenous trypsin inhibitor that prevents the auto-activation of prematurely activated trypsin (Whitcomb et al, 1996). Therefore, under physiological conditions, the acinar cell is well equipped to deal with aberrant enzyme activation. A breakdown in any or all of these mechanisms can initiate a pathological response resulting in a condition known as acute pancreatitis.

1.2 PANCREATITIS

Pancreatitis is an inflammatory disease that targets the exocrine pancreas. It affects 100,000 people in North America yearly and is often manifested in two forms: acute and chronic. Acute pancreatitis is identified by sudden onset, with symptoms being resolved within a short period of time and the pancreas returning to its normal functionality (Sarles et al, 1965; Steer & Meldolesi, 1988). 25% of patients with acute pancreatitis develop a severe form of the disease, which can be lethal in half of these cases (Bhatia, 2004). Characteristic symptoms of the disease include severe abdominal pain, nausea, diarrhea and fever. Histological analysis reveals inflammation of the pancreas evident from areas of lymphocyte infiltration, varying degrees of sclerosis, pancreatic and peri-pancreatic edema and occasional necrosis. Diagnostic tests for acute pancreatitis include an analysis of serum amylase and lipase levels, blood sugar levels, and subsequent histological examination of pancreatic morphology (Sarles *et al.*, 1965, Steer & Meldolesi, 1988).

Chronic pancreatitis is identified by persistent changes in pancreatic morphology and functionality, with long-term complications and recurring symptoms. It is believed to be a result of persistent attacks of acute pancreatitis episodes, causing irreparable damage to pancreatic morphology. Recurring attacks of significant steatorrhea (excessive fat content in stool) are a characteristic symptom. Histological changes in the pancreas include significant inflammation and lesions, extensive fibrosis and necrosis, occasional calcification and acinar dedifferentiation (Sarles et al, 1965).

1.2.1 Pathogenesis of pancreatitis

While the pathogenesis of acute pancreatitis is poorly characterized, the general consensus is that the initiating event involves the premature activation of enzymatic precursors, occurring within the acinar cell (Steer & Meldolesi, 1988). Recent evidence implicates the role of environmental stimuli in sensitizing the acinar cell to secretagogue input, including those of CCK and acetylcholine (reviewed by Gorelick & Thrower, 2009). Therefore, it appears that acute pancreatitis is a multi-factorial disease and the exact cause-effect relationship between application of harmful stimuli and initiation of the acinar response has not been unraveled. Nevertheless, some of the key events that occur in the earliest stages of acute pancreatitis pathogenesis have been well elucidated through the use of rodent models.

Although several models exist for studying the initiating events in pancreatitis, the best characterized model to date involves administration of supramaximal doses of the CCK analog, cerulein, via subcutaneous, intraperitoneal or intravenous routes of entry.

Cerulein-induced pancreatitis (CIP) induces a mild, edematous form of pancreatitis, with little to no mortality. In mice, CIP is induced by 1-10 hourly injections of cerulein and confirmed by significant increases in serum amylase and lipase levels, pancreatic edema and presence of acute pancreatic inflammation (Lampel & Kern, 1977). WT mice recover within 24 hours, as judged by return to normal serum enzyme levels and restoration of pancreatic tissue integrity (reviewed by Su et al, 2006).

Following induction of pancreatitis in the rodent pancreas with cerulein, one of the earliest morphological changes observed in the acinar cell is the formation and accumulation of vacuoles containing both digestive zymogens as well as lysosomal hydrolases (Watanabe et al, 1984; Saluja et al, 1987). This 'co-segregation' event allows for inactive digestive zymogens to come into contact with lysosomal hydrolases, particularly Cathepsin B, which has the ability to convert inactive trypsinogen to active trypsin (Saluja et al, 1985; Saluja et al, 1987). Premature activation of trypsinogen within the acinar cell is considered a hallmark of an early acute pancreatitis event. Activated trypsin can, in turn, activate other zymogens within the acinar cell, thereby initiating a cascade of events that leads to autodigestive injury to the pancreas (Greenbaum, Hirshkowitz & Shoichet, 1959; Figarella, Miszczuk-Jamska & Barrett, 1988). Other significant events in pancreatitis include a marked decrease in apical exocytosis and resulting release of activated enzymes into the interstitium, fragmentation of the Golgi apparatus, formation of autophagosomes, redistribution of the actin cytoskeleton, and upregulation of proinflammatory factors (Watanabe et al, 1984; Van Acker et al, 2007).

1.2.2 Environmental factors in pancreatitis

Several causes of pancreatitis have been identified, including alcohol abuse, ductal obstruction, ischemia and drugs (reviewed by Saluja & Bhagat, 2003). Among these, alcoholism and ductal obstruction by gallstones are the two leading causes of acute pancreatitis in humans (Ammann, 2001). In addition, cigarette smoking has been recently linked to acceleration of the progression of chronic pancreatitis in humans (Maisonneuve et al, 2005). Although the majority of cases of acute pancreatitis are associated with alcohol abuse, only a small percent of heavy alcohol abusers go on to develop pancreatitis (Saluja & Bhagat, 2003). Therefore, it is believed that genetics play a significant role in determining an individual's susceptibility and sensitivity to pancreatic injury.

1.2.3 Genetic susceptibility to pancreatitis

Given that the onset of pancreatitis is coincident with premature intracellular trypsinogen activation, studies have focused on the role of two genes in determining individual susceptibility to pancreatitis. A point mutation in exon 3 of the cationic trypsinogen gene, *PRSS1* results in persistent trypsin activity and correlates with the occurrence of hereditary pancreatitis in humans (Whitcomb et al, 1996). Estimated penetrance for mutations in *PRSS1* and the occurrence of hereditary pancreatitis is 80% (Whitcomb et al, 1996). More recent studies have also reported a high degree of correlation between mutations in *PSTI* (pancreatic secretory trypsin inhibitor) and the onset of pancreatitis (Witt et al, 2000). Analysis of a trypsin receptor of the protease-

activated receptor (PAR) family, PAR-2 has revealed that its activation, in concert with premature trypsinogen activation and its subsequent inhibition by *SPINK1* plays a role in the pathogenesis of acute pancreatitis (Maeda et al, 2005; Sharma et al, 2005). In addition, individuals with family history of hyperlipidemia, those with mutations in lipoprotein lipase (LPL) and those with apolipoprotein C II deficiency are at increased risk of developing acute pancreatitis (Wilson et al, 1993; Simon et al, 2001). Upon induction of pancreatitis, LPL deficient mice develop severe pancreatic necrosis and haemorrhaging as a result of free fatty acids in the blood (Wang et al, 2009). Rosendahl et al (2008) determined that among 908 individuals diagnosed with either idiopathic (etiology unknown) or hereditary pancreatitis, 4.8% contained *CTRC* (chymotrypsinogen C; a digestive enzyme with the ability to destroy prematurely activated trypsin) variants compared to 0.7% of healthy controls. While these findings underline the role of genetic factors in determining susceptibility to pancreatitis, they do not account for the majority of the genetic variation that increases susceptibility to pancreatitis.

1.3 ALCOHOL AND THE PANCREAS

Chronic alcohol abuse is a leading cause of health issues in North America, increasing the risk of liver disease, hypertension, and cancer. In addition, excessive alcohol consumption accounts for approximately 40% of all cases of chronic and acute pancreatitis. While the effects of alcohol on the acinar cell have been well characterized, the pathogenesis of alcohol induced pancreatitis is poorly understood. Studies in

rodents indicate that alcohol administration on its own has little to no effect on pancreatic morphology (Siech, Heinrich & Letko, 1991; Andrzejewska, Dlugosz & Jurkowska, 1998). Combining models of experimental pancreatitis with ethanol feeding indicates that ethanol sensitizes acinar cells to further damage. Rats fed an ethanol diet and subsequently injected with physiological doses of the cholecystokinin octopeptide (CCK-8) exhibited signs of pancreatitis that were absent in non-ethanol fed counterparts (Pandol et al, 1999; Pandol et al, 2003). This model allows for studying the effects of alcohol on pancreatic blood flow and acinar cell specific damage (reviewed by Schneider, Whitcomb & Singer, 2002).

1.3.1 Ethanol metabolism in the pancreas

Ethanol metabolism is said to occur predominantly via the oxidative or non-oxidative pathways. The oxidative pathway is catalyzed by the enzymes alcohol dehydrogenase, cytochrome P4502E1 (CYP2E1) and catalase, yielding the toxic metabolite, acetaldehyde and reactive oxygen species (ROS). In the non-oxidative pathway, ethanol is esterified by fatty acids, resulting in the production of cholesteryl esters (CE) and fatty acid ethyl esters (FAEE) as toxic metabolites (Haber et al, 1998). Ethanol metabolism by pancreatic acinar cells has been well characterized (Haber et al, 1998; Gukovskaya et al, 2002). Both, isolated pancreatic acinar cells and pancreatic tissue in vivo show similar activities of enzymes involved in ethanol processing, indicating that acinar cells are the source of ethanol metabolism in the pancreas. While ethanol is typically processed via the oxidative pathway in the liver, it is metabolized via

both pathways in the pancreas (Haber et al, 1998; Gukovskaya et al, 2002). However, alcohol dehydrogenase (ADH; the enzyme that catalyzes the conversion of alcohol to acetaldehyde) activity in the pancreas is only 7-12% of that in the liver while FAEE synthase activity is 4 times greater in the pancreas (Gukovskaya et al, 2002). On the other hand, in vitro studies have revealed that the rate of oxidative metabolism in the pancreas is significantly higher than that of non-oxidative metabolism (Apte et al, 1997; Gukovskaya et al, 2002). Taken together, it is clear that pancreatic acinar cells metabolize ethanol via both pathways, although the contributions of each pathway are not entirely understood.

Regarding the actions of the toxic metabolites of ethanol on the acinar cell, it has been established that acetaldehyde can cause morphological damage to rat and dog pancreatic acinar cells (Nordback et al, 1991). In addition, acetaldehyde has been shown to alter the acinar redox state, disrupt the actin cytoskeleton and alter CCK induced acinar enzyme secretion in vivo by affecting secretagogue binding to their receptors (Sankaran et al, 1985). ROS produced by oxidative metabolism have been linked to the generation of oxidant stress within the acinar cell, potentially resulting in damage to cell membranes and intracellular proteins (Norton et al, 1998). Both, acute and chronic exposure to ethanol results in the production of ROS, leading to oxidant stress in the rat pancreas (Norton et al, 1998). In vivo introduction of FAEEs into rats led to the development of pancreatic edema, formation of vacuoles within acinar cells, lysosomal destabilization and premature trypsinogen activation, events that are hallmarks of acute pancreatitis (Haber et al, 1993; Werner et al, 1997). Recent studies

have also elucidated the role of signalling pathways in mediating the effects of the toxic metabolites of ethanol on the acinar cell. For example, FAEE production has been shown to induce inflammatory signalling pathways involving the pro-inflammatory factors, nuclear factor –Kappa B (NF-kB) and activator protein-1 (AP-1), in addition to altering intracellular Ca^{2+} signalling pathways (Gukovskaya et al, 2002; Criddle et al, 2006). These findings suggest that ethanol metabolism in the pancreas plays a crucial role in determining its toxic effects on the acinar cell, thereby providing more insight into the pathogenesis of alcohol induced pancreatitis.

1.3.2 Models of alcohol induced pancreatitis

Animal models of ethanol intake have been a significant tool in studying the effects of ethanol on a variety of organs, particularly the liver, pancreas and the heart. In vitro models of acute ethanol exposure involve treatment of isolated pancreatic acinar cells with varying doses of ethanol, followed by examination of parameters of acinar function and/or injury (Cosen-Binker et al, 2007). Acute in vivo models include infusion (by catheters) of ethanol for a short duration and subsequent analysis. These systems have revealed the generation of plasma and pancreatic FAEEs and dose-dependent pancreatic injury, indicative of acute pancreatitis (Werner et al, 2002). Conventional chronic models include ethanol-laced diet models (as in the Lieber-DeCarli liquid ethanol diet), continuous intra-gastric infusion of ethanol (as in the Tsukamoto-French method), ethanol inhalation, ethanol gastric gavage and intraperitoneal injections (Lieber & DeCarli, 1986; reviewed by Keane & Leonard, 1989; Sampson et al, 1997;

Juarez & Barrios de Tomasi, 1999; Iumuro et al, 2000). Among these, the Lieber-DeCarli diet model is the most nutritional and physiologically relevant, with blood ethanol levels being equivalent to those observed during clinical intoxication in human patients (Lieber & DeCarli, 1986). The afore-mentioned models are not physiologically relevant due to the unconventional and physiologically irrelevant method of ethanol administration. On the other hand, a concern with the efficacy of the Lieber-DeCarli model is that dietary manipulation of the control diet to match calories in the ethanol diet may skew nutrient composition and yield nutrient-specific effects in controls. For instance, one variety of Lieber-DeCarli liquid control diet replaces calories from ethanol with 47% calories from carbohydrates while the isocaloric liquid ethanol diet is composed of only 11% from carbohydrates, making it a low-carbohydrate diet. In this instance, ethanol-specific effects are difficult to unmask (Lieber & DeCarli, 1986). Another criticism is the discrepancy in weight gain and preference for the diet in comparison to the controls. Despite its drawbacks, the Lieber-DeCarli diet model is still an effective and commonly used model system for studying alcohol induced pancreatitis.

1.3.3 Ethanol and pancreatic enzyme secretion

According to the current model of alcohol induced pancreatitis (**Figure 1.2**), ethanol is said to have two major effects on pancreatic enzyme secretion. A four –week liquid ethanol diet in rats resulted in a modest increase in protein and mRNA levels of the digestive enzymes, trypsinogen and chymotrypsinogen with statistically significant increases in pancreatic lipase as well as the lysosomal enzyme cathepsin B (Apte et al,

1995). Given that cathepsin B is capable of converting trypsinogen to trypsin within the acinar cell (Apte et al, 1995). Conversely, chronic ethanol intake in vivo in rats led to a decrease in basal rates of amylase secretion (Ponnappa et al, 1987). Chronic ethanol consumption followed by postprandial cholinergic stimulation results in a blocking of exocytosis at the apical pole and redirection to the basolateral aspect of pancreatic acinar cells (Cosen-Binker et al, 2007). Acute low-dose ethanol exposure, followed by cholinergic stimulation resulted in decreased amylase secretion from basal levels (Cosen-Binker et al, 2007). These findings suggest that ethanol consumption alters pancreatic enzyme secretion and potentiates the acinar cell to premature enzyme activation, thereby increasing susceptibility to the initiating events of acute pancreatitis.

Figure 1.2. Current model of the pathogenesis of alcoholic pancreatitis. According to the current hypothesis, ethanol and its toxic metabolites exert three major effects on the pancreatic acinar cell. Firstly, ethanol causes an increase in digestive (trypsinogen, chymotrypsinogen and lipase) and lysosomal enzyme (cathepsin B) content at both the mRNA and protein levels. Secondly, accumulation of ethanol's toxic metabolites such as cholesteryl esters (CEs) and fatty acid ethyl esters (FAEEs) cause the destabilization of lysosomes (L) and zymogen granules (ZG). Thirdly, in the presence of an appropriate trigger or co-factor, the acinar cell is sensitized to premature intracellular enzymatic activation, leading to inflammation, pancreatic stellate cell activation and fibrosis.

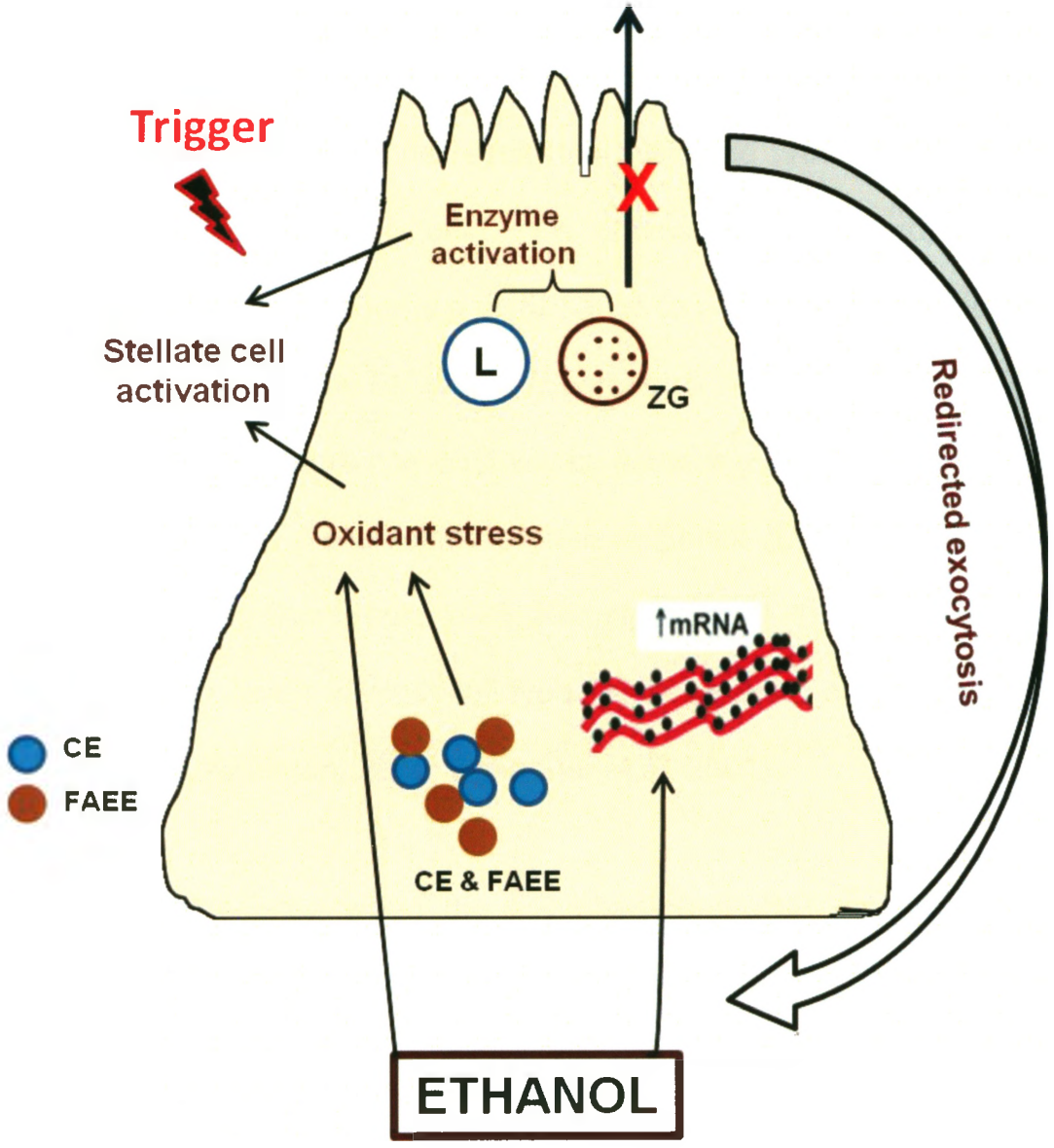

Adapted from Vonlaufen et al, 2007.

1.4 UNFOLDED PROTEIN RESPONSE

Protein folding in the endoplasmic reticulum is an intricate process carried out by two main classes of proteins: chaperones and foldases (Schroder & Kaufman, 2006). When this process is disrupted, the result is a misfolded protein, mainly characterized by exposed hydrophobic amino acid side chains that can form aggregates and accumulate in the ER. This presents a disturbance to physiological ER homeostasis and results in a condition known as ER stress (Schroder & Kaufman, 2006). The ER aims to alleviate ER stress and restore homeostasis by activating signal transduction pathways, collectively referred to as the unfolded protein response (UPR; Adams & Rose, 1985; Gething, McCammon & Sambrook, 1986; Kozutsumi et al, 1988). In addition, the UPR is also active at basal levels in most cell types in response to changes in nutrient levels (Schroder, Chang & Kaufman, 2000; Scheuner et al, 2001).

The UPR is initiated when the ER chaperone, BiP (immunoglobulin binding protein)/GRP78 (Glucose regulated protein 78) dissociates from the three main transducers of ER stress, namely PERK (protein kinase R (PKR) like endoplasmic reticulum resident kinase), IRE1 (inositol-requiring enzyme 1) and ATF6 (activating transcription factor 6) (**Figure 1.3**) (Adams & Rose, 1985; Gething, McCammon & Sambrook, 1986).

Figure 1.3. Schematic of the mammalian unfolded protein response. The UPR comprises three signal transduction pathways and is initiated when the ER chaperone, BiP/GRP78 dissociates from the three main transducers of ER stress, PERK, IRE1 and ATF6. Upon release of BiP, PERK undergoes oligomerization and autophosphorylation and phosphorylates its substrate, eIF2α, which in turn causes an increase in translation of ATF4 and its target ATF3. Activation of the PERK arm results in a general attenuation of protein translation. Prolonged ER stress can activate the pro-apoptotic factor, CHOP which in turn can induce GADD34 expression. GADD34 acts in a negative feedback fashion by associating with PP1 to promote dephosphorylation of eIF2α. Upon activation, IRE1 oligomerizes and trans-autophosphorylates, allowing it to cleave a 26-bp fragment from the mRNA of its substrate, *Xbp1*. sXBP1 is a potent transcription factor that induces expression of ER chaperones and foldases. Activation of ATF6 results in its cleavage in the Golgi and translocation to the nucleus where it induces expression of ER chaperones and factors that degrade the unfolded/misfolded proteins.

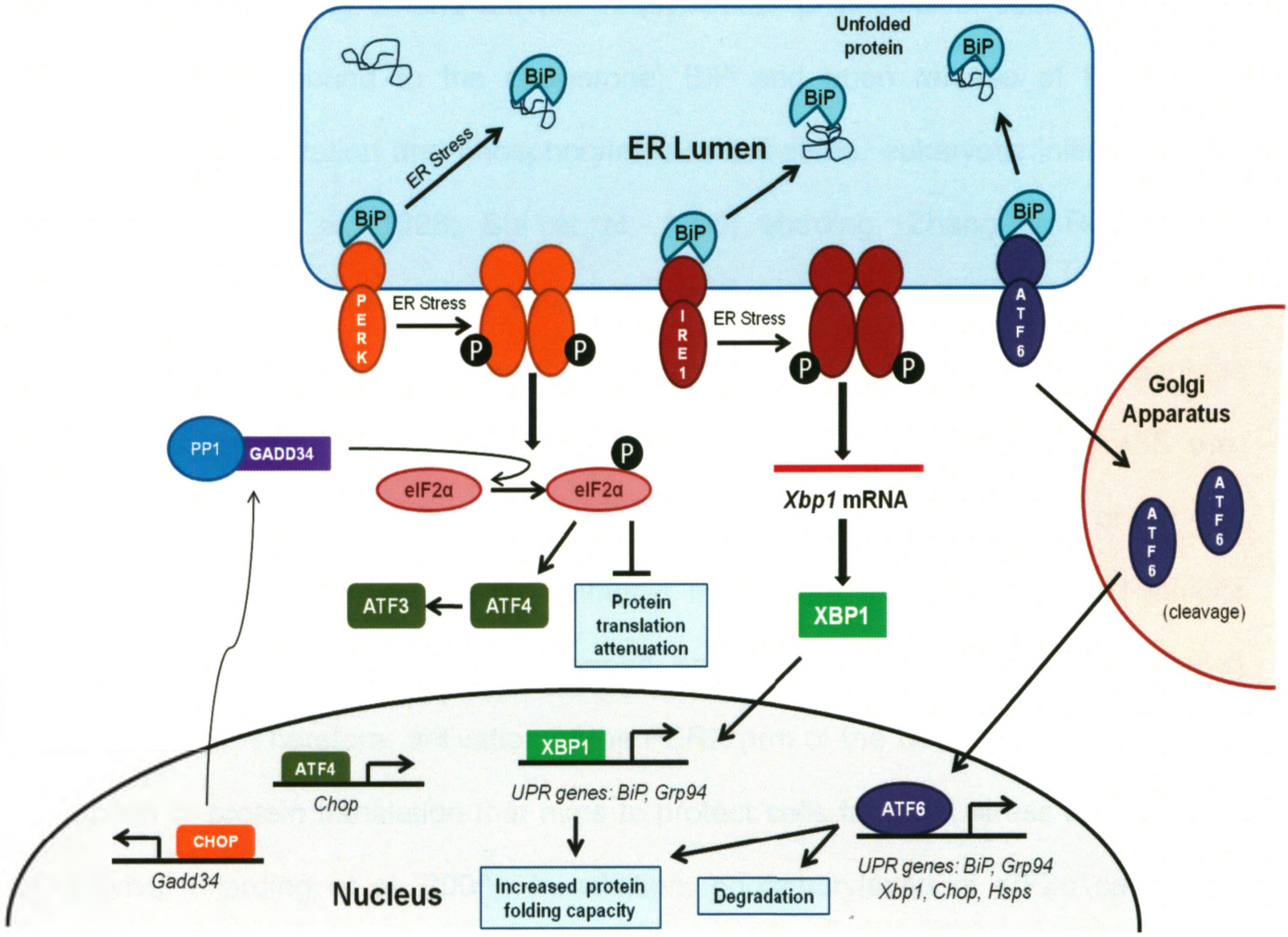

Adapted from Schroder & Kaufman, 2004.

1.4.1 The PERK Pathway

PERK is an ER resident type I transmembrane protein kinase (Shi et al, 1998; Shi et al, 1999; Harding, Zhang & Ron, 1999). Under physiological conditions, its ER luminal domain is bound to the chaperone, BiP and upon release of BiP, PERK undergoes oligomerization and phosphorylates its substrate, eukaryotic initiation factor 2α (eIF2α) (Shi et al, 1998; Shi et al, 1999; Harding, Zhang & Ron, 1999). Phosphorylation of eIF2α on the serine 51 residue (Harding, Zhang & Ron, 1999) causes the inhibition of guanosine-5'-triphosphate (GTP)- guanosine-5'-diphosphate (GDP) exchange on eIF2 by eIF2β, thereby preventing formation of the 43S pre-initiation complex (Schröder & Kaufman, 2006). This complex is comprised of the 43S ribosomal subunit, GTP, eIF2 and methionyl methionine initiator tRNA and inhibits translation upon its entry to the 5' capped end of eukaryotic mRNA (Schröder & Kaufman, 2006). Therefore, activation of the PERK arm of the UPR results in a general attenuation of protein translation that aims to protect cells from ER stress and promote cell survival (Harding et al, 2000). In addition, phosphorylation of eIF2α causes an increase in translation of activating transcription factor 4 (ATF4) by selective translation of mRNAs encoding for upstream open reading frames (uORFs) (Hinnebusch, 1997; Harding et al, 2000). ATF4 can induce expression of the transcription factor ATF3 (activating transcription factor 3; a member of the ATF/CREB subfamily of basic-region leucine zipper (bZIP) proteins), which in turn induces expression of the pro-apoptotic transcription factor CHOP (CCAAT/enhancer binding protein homologous protein) and GADD34 (growth arrest and DNA damage inducible protein 34) (Jiang et al, 2004). Activation of the PERK pathway in response to ER stress is tightly regulated. *Gadd34*

associates with the catalytic subunit of protein phosphatase 1 (PP1; an eIF2α phosphatase) and promotes the dephosphorylation of eIF2α in negative feedback fashion to control the attenuation of translation response to PERK activation (Connor et al, 2001).

Analysis of a *Perk*$^{-/-}$ mouse model has revealed a significant effect on the exocrine pancreas. *Perk*$^{-/-}$ mice show significant acinar cell death and atrophy of the pancreas three weeks postnatally (Zhang et al, 2002). There is a loss of endocrine pancreatic β cells and a subsequent diabetic phenotype due to deficiencies in insulin production as well as defects in bone formation (Harding et al, 2001; Zhang et al, 2002). In addition, the acinar cell specific *Perk*$^{-/-}$ mouse revealed that the effects of PERK on the exocrine pancreas are cell-autonomous and the deficits observed are not due to ER stress, but rather an inflammatory response that leads to an oncotic (swelling necrosis) form of cell death (Iida et al, 2007).

1.4.2 The IRE1 pathway

IRE1 is an ER resident type I transmembrane protein kinase with endoribonuclease activity (Cox, Shamu & Walter, 1993; Mori et al, 1993). Mammals contain two isoforms of IRE1 - IRE1α (Tirasophon et al, 2000) and IRE1β (Wang et al, 1998). The luminal N-terminal domain of IRE1 senses accumulation of unfolded or misfolded proteins in the ER. Release of the ER chaperone BiP is the triggering event for activation of IRE1 upon induction of ER stress (Cox, Shamu & Walter, 1993). The C-terminal domain of IRE1 is an RNAse (endoribonuclease) whose known substrate in

yeast is *HAC1* mRNA, the functional homologue to mammalian *XBP1* (X-box binding protein 1) (Yoshida et al, 2001; Calfon et al, 2002). Upon activation, IRE1 oligomerizes and trans-autophosphorylates its kinase domain, thereby opening its ATP-binding domain (Papa et al, 2003). Binding of ADP to this domain is sufficient to cause an activating conformational change in the RNAse domain of IRE1, allowing it to cleave exon-intron junctions in the mRNA of its substrates (Cox, Shamu & Walter, 1993; Yoshida et al, 2001; Calfon et al, 2002; Papa et al, 2003). In yeast, tRNA ligase splices the exons of $Hac1^{u}$ (uninduced *Hac1*) mRNA while in mammals, an *Xbp1* ligase is yet to be identified (Sidrauski, Cox & Walter, 1996). The resulting transcripts: $Hac1^{i}$ (induced *Hac1*) in yeast and *sXbp1* (spliced *Xbp1*) in mammals are actively translated to transcription factors that translocate to the nucleus and regulate expression of several UPR target genes (including ER chaperones and factors that promote ER associated degradation) by binding to specific promoter regions such as the UPRE (unfolded protein response element) and ERSE-1 (ER stress response element 1) (Mori et al, 1998; Yoshida et al, 2001).

Recent studies have highlighted the role of XBP1 in the exocrine pancreas. Pancreatic acinar cell specific ablation of XBP1 has been demonstrated to be lethal to acinar cells, resulting in ER stress, loss of zymogen granules (and MIST1 expression) and acinar ultra-structure, reduction in the enzymes, amylase and elastase and premature activation of the digestive enzyme, carboxypeptidase (CPA) (Hess et al, 2011). Remarkably, following the acinar cell specific ablation of XBP1, the pancreas showed a regenerative response involving progenitor centroacinar cells (Hess et al,

2011). These findings implicate XBP1 not only as a key regulator of ER stress in the pancreas but also in the maintenance of acinar cell viability (Hess et al, 2011).

Ire1$^{-/-}$ mice have been characterized and were found to be lethal between embryonic days 9.5 to 11.5 (Urano et al, 2000). *Xbp1*$^{-/-}$ mice on the other hand also begin to die at embryonic day 12.5 primarily through defective plasma cell and hepatocyte differentiation (Reimold et al, 2000), suggesting that these two molecules play an integral role in development in addition to their function as mediators of ER stress.

1.4.3 The ATF6 pathway

Activating Transcription Factor 6 (ATF6) is a type II transmembrane bZIP transcription factor that has two isoforms - ATF6α and ATF6β (Haze et al, 2001). During ER stress, BiP dissociates from ATF6 at which time, ATF6 translocates from the ER membrane to the Golgi apparatus where it undergoes sequential cleavage of its luminal domain by the Golgi resident serine protease, S1P (site 1 protease) (Haze et al, 1999; Yoshida et al, 2000). The metalloprotease, S2P (site 2 protease) then cleaves and releases the cytosolic N terminal domain of ATF6 (Haze et al, 1999; Yoshida et al, 2000; Ye et al, 2000). The cleaved ATF6 then translocates to the nucleus where the cytosolic domain binds to the ATF/cAMP response element (CRE) and the ER stress response elements (ERSE) I and II (Yoshida et al, 1998; Wang et al, 2000; Kokame, Kate & Miyata, 2001). Targets of ATF6 include ER resident molecular chaperones (such

as BiP), and transcription factors XBP1 and CHOP (Wang et al, 2000). These factors aim to restore protein folding and alleviate ER stress.

Atf6α$^{-/-}$ mice show no overt phenotype under non-stress conditions, but upon induction of ER stress by tunicamycin (a chemical agent that inihibits N-linked protein glycosylation and generates ER stress), these mice develop hepatic steatosis (Wu et al, 2007). *Atf6β*$^{-/-}$ mice show normal development and no overt phenotype, while *Atf6α*$^{-/-}$ */Atf6β*$^{-/-}$ mice exhibit embryonic lethality, indicating redundancy in the functions of the two molecules (Yamamoto et al, 2007). These findings suggest that while the two isoforms of ATF6 are not individually crucial for development, they play a critical role in maintaining ER function during chronic stress.

Persistent ER stress can lead to activation of cell death mechanisms, particularly through the apoptotic pathway. Failure to ameliorate ER stress is believed to cause a switch from the immediate adaptive responses to a multitude of intrinsic and extrinsic pro-apoptotic responses. One prominent route is through the transcriptional induction of *Chop* separately by ATF6 and ATF4 (Scheuner et al, 2001; Oyadomari & Mori, 2004). Additionally, the IRE1 pathway of the UPR can activate apoptotic cell death. IRE1 forms a complex with TRAF2 (tumour necrosis factor receptor associated factor 2) and ASK1 (apoptosis signal-regulating kinase 1) to activate c-Jun amino-terminal kinase to induce apoptosis (Urano et al, 2000). Nevertheless, the dynamics of this switch from anti- to pro-apoptotic mechanisms remain unclear. The UPR is hence a complex signalling pathway playing a dual role in protecting the cell from stressors. On the one hand, the adaptive aspect of the UPR aims to alleviate ER stress and restore homeostasis by

attenuating protein translation, upregulating ER chaperones and promoting ER associated degradation of misfolded proteins. On the other hand, chronic and severe ER stress promotes cell death via apoptosis.

It is possible that mutations in UPR mediators, acting in concert with environmental stressors predispose some individuals and not others to pancreatic disease (reviewed by Pandol et al, 2011). For instance, certain *Xbp1* mutations confer risk for inflammatory bowel disease in humans (Kaser et al, 2008). While all three pathways of the UPR are activated in response to both L-arginine and cerulein-induced pancreatitis (Sans et al, 2003; Kubisch et al, 2006; Kowalik et al, 2007), the role of ER stress in the pathogenesis of pancreatitis has not been fully characterized. A number of gene targets have been identified for sXBP1, including *Mist1*, a basic helix-loop-helix (bHLH) transcription factor required for complete acinar cell maturation (Pin et al, 2001; Alcosta-Alvear et al, 2007). Given that chronic ethanol feeding induces *Xbp1* splicing, this project examines UPR activity in response to chronic ethanol exposure, in the context of a *Mist1*$^{-/-}$ mouse model.

1.5 MIST1 AND THE PANCREAS

MIST1 is a serous exocrine cell specific transcription factor that is crucial for the complete maturation and proper function of acinar cells of the exocrine pancreas (Pin et al, 2001; Johnson et al 2004). It is also required for intracellular organization of acinar cells and as a consequence, regulated exocytosis (Johnson et al, 2004). MIST1 expression is first observed in the nuclei of acinar cells of the developing pancreas at

embryonic day 10.5 (Pin et al, 2001). It is completely absent from endocrine and ductal pancreatic tissue (Pin et al, 2001). In addition to the pancreas, *Mist1* is expressed in cells that exhibit regulated exocytosis, including the acinar cells of the salivary and lacrimal glands, chief cells of the stomach, Paneth cells of the intestine and secretory cells of the seminal vesicle and prostate gland (Pin et al, 2000). Our lab has generated a *Mist1*$^{-/-}$ mouse model to better understand the role of *Mist1* in pancreatic development, function and disease.

1.5.1 The *Mist1*$^{-/-}$ mouse

The *Mist1*$^{-/-}$ mouse shows no overt phenotype (Pin et al, 2001). They are viable and fertile and develop a functional pancreas (Pin et al, 2001). At the histological level, one of the most salient differences between WT and *Mist1*$^{-/-}$ pancreatic tissue is the disruption of both inter- and intracellular acinar organization in the *Mist1*$^{-/-}$ tissue. At the intracellular level, *Mist1*$^{-/-}$ cells have apparent mislocalization of the nucleus and ER and dispersed zymogen granules throughout the cell in contrast to the WT acinar cell with a basally localized nucleus and ER and apically localized zymogen granules (Pin et al, 2001). The primary deficit in the *Mist1*$^{-/-}$ pancreas is the inability to properly position zymogen granules at the apical pole of the acinar cell for regulated exocytosis (Johnson et al, 2004). *Mist1*$^{-/-}$ cells also show deficits in intracellular calcium signalling, including the presence of aberrant calcium waves in response to secretagogue stimulation and loss of IP_3R_3 (inositol tri-phosphate receptor 3) (Luo et al, 2005).

Mist1$^{-/-}$ tissue deteriorates over time, resulting in the loss of acinar cell differentiation characteristics and appearance of pancreatic lesions in older mice, including distended acinar and duct lumens (Pin et al, 2001). Part of the *Mist1*$^{-/-}$ phenotype includes premature activation of digestive enzymes such as carboxypeptidase (CPA) and subsequent intracellular digestion of organelles (Pin et al, 2001). These events are comparable to the initial events in the pathogenesis of pancreatitis. Furthermore, expression of genes that are known to be upregulated during pancreatitis, such as *PSP* (pancreatic stone protein) and *PAP1* (pancreatitis associated protein 1), is significantly increased in *Mist1*$^{-/-}$ tissue (Pin et al, 2001). These characteristics make the *Mist1*$^{-/-}$ mouse a model of chronic pancreatic injury and an important tool for studying the pathogenesis of pancreatitis.

1.5.2 The UPR in the *Mist1*$^{-/-}$ mouse

Following the initiation of cerulein induced pancreatitis, assays for key UPR markers revealed a number of striking differences between WT and *Mist1*$^{-/-}$ cells (**Figure 1.4**). After 4 hours of initial cerulein stimulation, *Mist1*$^{-/-}$ cells failed to show significant increases in ATF3 expression and phosphorylation of eIF2α, relative to WT cells. GADD34 levels were elevated before and after cerulein stimulation in *Mist1*$^{-/-}$ cells, suggesting an inhibition of eIF2α dephosphorylation. Taken together, these findings indicate that the *Mist1*$^{-/-}$ mouse is a genetic model of chronic stress with disregulation of the UPR upon induction of pancreatic injury.

Figure 1.4 Differential activation of the UPR in WT and *Mist1*$^{-/-}$ pancreatic acinar cells upon induction of acute pancreatic injury. Upon initiation of CIP, WT pancreatic acinar cells show activation of all three arms of the UPR. Following the release of BiP, PERK undergoes phosphorylation and oligomerization, resulting in the phosphorylation of eIF2α, causing a general attenuation of translation. This is regulated in a negative feedback fashion by GADD34, which promotes the dephosphorylation of eIF2α. Phosphorylated IRE1 increases ASK1 expression thereby activating JNK and promoting apoptotic cell death. *Mist1*$^{-/-}$ pancreatic acinar cells contain significantly high levels of GADD34 prior to CIP, preventing the phosphorylation of eIF2α and inhibiting translational attenuation in response to CIP. Limited JNK activation (decreased apoptosis) and ATF3 expression is observed, coincident with increased severity of pancreatitis.

WT Acinar Cell

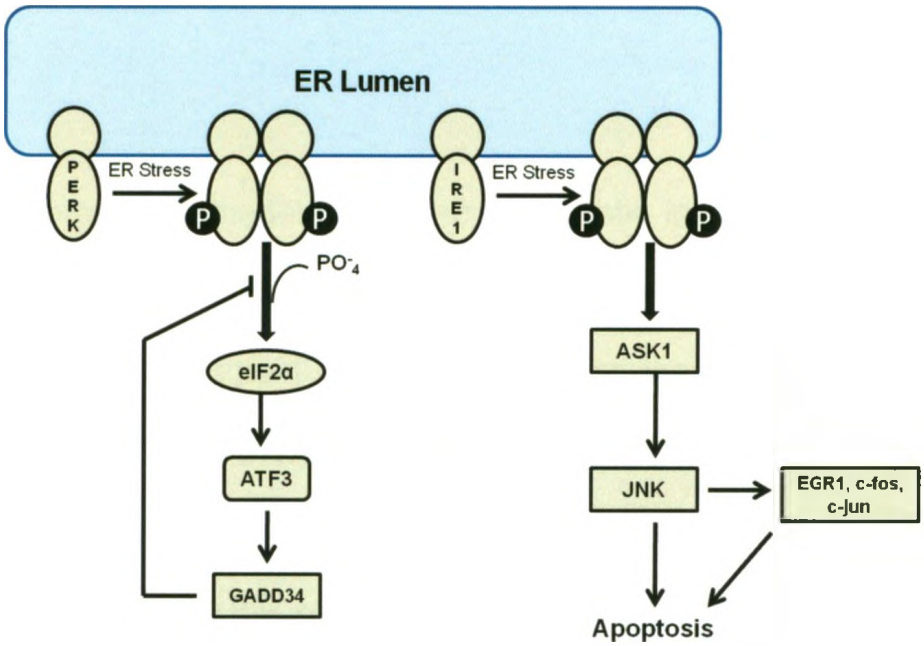

***Mist1*$^{-/-}$ Acinar Cell**

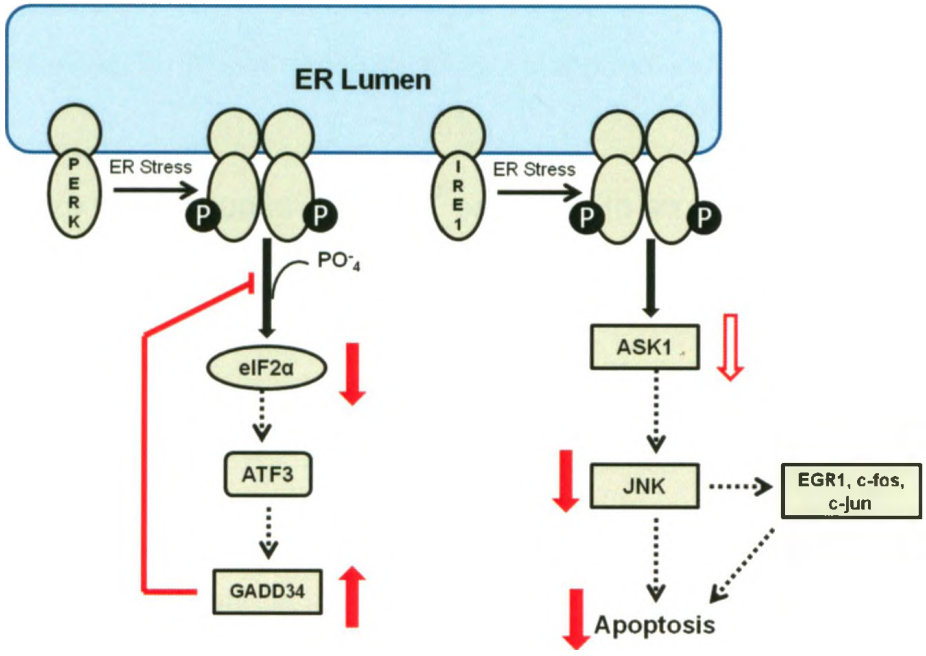

Adapted from Kowalik et al, 2007

1.6 HYPOTHESIS AND OBJECTIVES

Hypothesis

Mist1$^{-/-}$ mice represent a model of chronic pancreatic injury. Upon induction of acute pancreatitis, they show increased susceptibility to and severity of pancreatic damage and an altered unfolded protein response. Based on these studies, I hypothesize that *Mist1*$^{-/-}$ mice will be more sensitive to chronic ethanol feeding, compared to WT mice, due to an inability to fully activate the unfolded protein response. To address this hypothesis, I undertook the following objectives:

Objectives

1. Characterize the response of *Mist1*$^{-/-}$ pancreas to an ethanol laced diet
2. Examine the effect of chronic ethanol feeding on the UPR in pancreatic acinar cells
3. Examine the UPR in *Mist1*$^{-/-}$ pancreatic acinar cells following ethanol feeding
4. Determine if chronic ethanol feeding followed by induction of acute pancreatitis alters UPR in pancreatic acinar cells

This work should provide a better explanation of how MIST1 governs susceptibility to pancreatic disease during adverse dietary conditions.

CHAPTER 2: MATERIALS AND METHODS

2.1 ANIMALS

All mice used for this project were male and have a C57BL/6 genetic background. *Mist1*$^{-/-}$ mice were generated in which the coding region of both the endogenous *Mist1* alleles was replaced by the bacterial *LacZ* gene, which encodes for the enzyme, β-galactosidase (β-gal; Pin et al, 2001). *Mist1*$^{-/-}$ animals were backcrossed for ten generations to be congenic with C57BL6 mice.

Mice were handled according to the stipulations of the University of Western Ontario and by the Canadian Council for Animal Care. All procedures were approved by the Animal Care Committee at the University of Western Ontario (Protocol # 2008-116). Animals were housed in individual cages in a closed facility with a 12 hour light-dark cycle and fed standard rodent chow, except where indicated.

2.2 DIETS

Four to five month-old C57BL/6 *Mist1*$^{-/-}$ (Pin et al, 2001) and congenic C57 Bl6 mice were housed individually and fed a Lieber-DeCarli ethanol (LDC-E; diet #L10016, Research Diets) diet *ad libitum* for six weeks (n=5 (round 1); n=7 (round 2); n=4 (round 3)). This diet consisted of 36% of kcal from ethanol and 36% of kcal from fat. As a control, mice were fed a LDC-C liquid diet (diet #L10015, Research Diets) that replaced calories from ethanol with those from isocaloric maltodextrin (a carbohydrate). The LDC-C diet also consisted of 36% of kcal from fat. Control mice were fed standard

breeder's chow that had a lower composition of fat (22% kcal; Teklad Global 2019 Rodent Diet). During the course of the diet, mice were weighed daily and food replaced daily. Food intake was measured by subtracting the amount remaining in the feeding bottle following a 24 hour period from the amount that was initially placed. Daily caloric intake was determined with 1 gram of the diet equivalent to 1 mL and yielded 1 kcal of energy units. For comparison of diets, see Table 2.1.

2.3 INITIATION OF CERULEIN-INDUCED PANCREATITIS

In some mice, mild edematous acute pancreatitis was induced in mice following the 6 week LDC-C and LDC-E diet in wild type mice, through four hourly injections of cerulein. Control mice on the standard chow diet were also injected with cerulein. Each mouse received 50 µg/kg body weight of cerulein per injection (Sigma, St. Louis, MO) dissolved in 0.9% saline, via intraperitoneal injections (n=4).

2.4 SERUM AMYLASE ANALYSIS

Blood was obtained through cardiac puncture, placed on ice for 20 minutes and centrifuged at 5000 x g for 15 minutes at 4°C. Serum amylase levels were determined in the resulting serum, using the *Phadebas* amylase detection kit (Pharmacia Diagnostics, Dorval, QC) as per manufacturer's instructions.

2.5 EDEMA

A small portion of the pancreas was removed and placed into pre-weighed Eppendorf tubes, which were weighed along with the pancreas to obtain wet pancreatic weight. Tubes were incubated at 55^0C for 2 days, allowing for complete desiccation of the pancreas. The net water loss was determined by the following equation;

Edema (%) = (Wet weight – Dry weight] / [Wet weight]) x 100%

2.6 PROTEIN ANALYSIS

2.6.1 Protein Isolation and Quantification

At the time of dissection, the splenic portion of the pancreas was removed and immediately frozen in liquid nitrogen. Tissue was later homogenized and sonicated in isolation buffer consisting of 1 M Tris (pH 7.2), 1 M $MgCl_2$, 1 M $CaCl_2$, 1 M DTT, 5% (wt/vol) Nonidet P-40, 30 mM NaF, 2 mM NaVO, 5 µM Leupeptin, 5 µM Chymostatin, 5 µM Pepstatin, 1 mM PMSF and dH_20. Approximately 500 µL of the buffer was used per 100 mg of tissue. Homogenized samples were then sonicated for 20 seconds at high speed and centrifuged at 5000 x g for 5 minutes. The pellet was discarded and the supernatant was retained. Protein samples were then quantified using a Bradford protein quantification assay. In this assay, 1 mL of Bradford solution (4 parts dH_20 to 1 part Bradford dye (Bio-Rad, CA) was added to 1 µL protein sample. This solution was allowed to stand at room temperature for 15 minutes before its absorbance was determined by a spectrophotometer (set at wavelength 590 nm). The resulting

absorbance values were converted to concentrations in µg/µL according to the following calculation:

$$\text{Concentration (µg/µL)} = [\text{Absorbance} \times 0.038] / 0.07$$

2.6.2 Immunoblotting

For immunoblot analysis, 40-50 µg of protein was resolved by Sodium Dodecyl Sulfate-Polyacrylamide Gel Electrophoresis (SDS-PAGE). For this procedure, 7-12% acrylamide solutions were prepared and poured between glass plates, combined into a plate holding assembly. The separating gel consisted of a buffer consisting of Tris, SDS and dH_2O (pH 8.8), acrylamide stock and distilled water along with 10% ammonium persulfate (APS) and tetramethylethylenediamine (TEMED). Following polymerization for 30 minutes, a stacking gel composed of a buffer consisting of Tris, SDS and dH_2O (pH 6.8), acrylamide stock, distilled water, 10% APS and TEMED was pipetted onto the separating gel. A 10 or 15 well comb was inserted to form wells in the stacking gel. For preparation of the protein samples, 5µL of 1x SDS loading dye was added to 1µL of β-mercaptoethanol and the appropriate volume of protein, as determined by its concentration. Samples were heated at 95^0C and centrifuged before being loaded onto wells. Protein was resolved on the gel at 100 volts until the dye front reached the end of the gel.

Following electrophoresis, 10 µg of protein was resolved by SDS-PAGE as previously described (see section 2.5.2). After electrophoresis, the gel was incubated with Coomassie blue stain for 30 minutes followed by incubation with a destain solution for

another 30 minutes. Gels were then imaged using the VersaDoc imaging system (Bio-Rad model 3000) under white light. Alternatively, protein was transferred to a polyvinylidene difluoride (PVDF) membrane (Bio-Rad, Hercules, CA) via wet transfer, at 200 mA for 90 min. The membrane was incubated with blocking buffer (5% non-fat dry milk in phosphate buffered saline [PBS] with 0.1% Tween; PBS-T) for 30 minutes, followed by incubation with primary antibody diluted in blocking buffer for 1 hour, three washes in PBS-T and incubation with secondary antibody diluted in blocking buffer for one hour. For analysis of proteins such as BiP, pPERK and peIF2α, the blocking buffer consisted of 5% Bovine Serum Albumin (BSA) in TBS with 0.1% Tween, whereas the primary antibody was diluted in 5% BSA with gentle shaking at 4°C overnight. Following five more washes with PBS-T, the membrane was incubated in enhanced chemiluminescent substrate (Perkin Elmer, Woodbridge, ON) and exposed to X-ray film in a dark room. Alternately, the membrane was imaged using the VersaDoc imaging system (Bio-Rad model 3000) on the chemiluminscence channel and subsequently analyzed.

2.6.3 Densitometry

Densitometric analysis was performed on images obtained on the VersaDoc imaging system using ImageLab Software (Bio-Rad). Artificial bands were overlaid onto the protein bands in the image and adjusted accordingly. Band volumes were determined by the software based on relative pixel intensities.

2.6.4 Antibodies

Primary antibodies used included rabbit antibodies directed against amylase (dilution 1:1000; Calbiochem, San Diego, CA), ATF3 (1:500; Santa Cruz Biotechnologies, Santa Cruz, CA), ATF4 (1:500; Santa Cruz), ATF6 (1:500; Santa Cruz), Carboxypeptidase (1:1000; Cedarlane Laboratories, Hornby, ON), BiP (1:1000; Cell Signalling Technology, Pickering, ON), eIF2α (1:500; Cell Signalling), GADD34 (1:500; Santa Cruz), LC3I/III (1:500; Cedarlane), pPERK (1:500; Cell Signalling), peIF2α (1:500; Cell Signalling) and total XBP1 (1:500; Santa Cruz) and β-actin (1:500; Santa Cruz). Secondary antibodies were conjugated to horse radish peroxidase (HRP; 1:10,000; Sigma, St. Louis, MO). See Table 2.2 for a list of antibodies

2.6.5 Western membrane stripping

Following visualization of protein, membranes were kept at 4^0C until they were ready for stripping. The membrane was washed in PBS-T twice for 10 minutes each and incubated in a stripping buffer consisting of (β-mercaptoethanol, 0.5 M Tris-HCl pH 6.8, 10% SDS and dH_20) at 60^0C for 30 minutes. This was followed by three more washes in PBS-T for 10 minutes each after which it was ready to be blocked.

2.7 RNA ISOLATION

Total RNA was isolated using TRIzol® reagent (Invitrogen), from the duodenal portion of the pancreas as follows. Approximately 50 mg of pancreatic tissue was homogenized in 5 mL of TRIzol® reagent and incubated in ice for 5 minutes. Chloroform was added to this solution (0.2 mL per 5 mL Trizol) followed by incubation in ice for 3 minutes and

centrifuging at 5000 rpm (4^0C) for 15 minutes. The RNA aqueous phase was removed and added to 0.5 mL of isopropanol per 5 mL Trizol which was then incubated at -20^0C for 30 minutes. The mixture was then centrifuged at 5000 rpm (4^0C) for 15 minutes and the supernatant removed. The resulting RNA pellet was washed in 1 mL 75% ethanol in RNAse free diethylpyrocarbonate (DEPC) dH_2O and centrifuged at 5000 rpm (4^0C) for 15 minutes. The supernatant was removed and the RNA pellet was air dried and re-dissolved in 100-300 µL RNAse free DEPC dH_2O and stored at -80^0C. RNA concentrations (in ng/µL) were determined using a NanoDrop 3300 fluorospectrophotometer (NanoDrop Technologies, Thermo Fisher Scientific, Ottawa, ON).

2.8 RT PCR & AGAROSE GEL ELECTROPHORESIS

2 µg of total mRNA was transcribed to cDNA in the presence of random primers in DEPC dH_2O and heated at 70^0C for 10 minutes and quickly chilled on ice for 5 minutes. This mixture was then added to a master mixture composed of 5 x first strand buffer, 25 mM $MgCl_2$ and 10 mM dNTPs in DEPC dH_2O. 1 µL of the enzyme reverse transcriptase was added and the resulting mixture was heated at 42^0C for 1 hour, 70^0C for 15 minutes and chilled on ice for 5 minutes.

PCR (Polymerase Chain Reaction) was performed with 1 µL cDNA (obtained from RT reactions) in 24 µL master mix, consisting of 2.5 µL of buffer, 1 µL of 0.25 mM $MgCl_2$, 0.5 µL dNTPs, 0.5 µL of 3' and 5' primers and 18.75 µL dH_2O per reaction. 0.25 µL of

Taq polymerase was added to this mixture at the time of PCR. The reaction was carried out on an Eppendorf Mastercycler® (Eppendorf, Germany).

Primers to amplify Xbp1 and *β-actin* were based on sequences obtained from NCBI (http://www.ncbi.nlm.nih.gov/tools/primer-blast). Primer sequences to amplify *Xbp1* were:

Xbp1 forward: 5' AAACAGAGTAGCAGCGCAGACTGC 3'

Xbp1 reverse: 5' TCCTTCTGGGTAGACCTCTGGGAG 3'

These primers produced amplicon sizes of 289 bp and 263 bp for *uXbp1* and *sXbp1* respectively. To calculate the ratio of *sXbp1* to *uXbp1*, pixel intensity of the *sXbp1* band was divided by the pixel intensity of the *uXbp1* band, obtained using ImageLab software (Bio-Rad) following visualization in the VersaDoc imaging system (Bio-Rad).

Primer sequences to amplify for *β-actin* were:

β-actin forward: 5' ATGGAGAAGATCTGGCAC 3'

β-actin reverse: 5' CGTCACACTTCATGATGG 3'

These primers produced amplicon sizes of 212 bp.

The PCR product was subsequently analyzed on a 1-3% agarose gel (agarose dissolved in Tris base, acetic acid and EDTA (TAE) buffer and ethidium bromide) at 100-120 volts for 40 minutes. The gel was visualized using the GelDoc system under ultraviolet light.

2.9 HISTOLOGY

2.9.1 Sectioning

Following dissection, the duodenal portion of the pancreas was removed and placed into OCT (Shandon cryomatrix solution; Thermo Fisher Scientific) and immediately frozen in liquid nitrogen. Frozen sections were later sectioned to 7 µm using a Shandon cryostat (Thermo Fisher Scientific). For histological analysis, pancreatic tissue was rinsed in PBS, fixed in 4% formaldehyde for 24 hours and processed for paraffin sectioning (VRL Histocore facility, London, ON).

2.9.2 H&E Staining

Hematoxylin and Eosin (H&.E) staining was performed on frozen cryosections. Slides were first rehydrated in 70% ethanol and tap water, stained with CAT hematoxylin (Biocare), blueing solution and Eosin Y respectively. The dehydration step involved rinses in 70, 90 and 100% ethanol consecutively before repeated washes in xylene and mounting onto slides. CAT hematoxylin stains basophilic cellular structures while eosin stains the eosinophilic structures.

2.9.3 Trichrome Staining

Paraffin sections were sent to Robarts Research Institute (University of Western Ontario, Canada) for Gomori's trichrome staining. According to this protocol, connective tissue is stained in blue the nuclei are stained in purple and the cytoplasm in dark red.

2.9 IMMUNOFLUORESCENCE

Slides with cryosectioned pancreatic tissue were allowed to thaw for 10 minutes before being fixed with 4% formaldehyde. After washes in PBS, 0.1% Triton-X in PBS was added to permeabilize the cell membrane, for 15 minutes. More washes in PBS were followed by incubation in blocking solution for 30 minutes, consisting of 5% BSA in 0.1% Triton-X in PBS to prevent non-specific binding of antibodies. Sections were then incubated in primary antibody in blocking solution for 1 hour, washed in blocking solution and incubated in secondary antibody in blocking solution for 1 hour. More washes in PBS were followed by incubation in DAPI (4', 6-diamidino-2-phenylindole; 1:500 for 5 minutes to stain DNA. Slides were washed in PBS and then coverslipped with VECTASHIELD® mounting media (Vector Laboratories).

2.9.1 Antibodies

Primary antibodies used included rabbit antibodies directed against CD4 (1:500; BD Pharmingen, Mississauga, ON) and LC3I/II (1:500; Cell Signalling). Secondary antibodies were conjugated to either fluorescein iso-thiocyanate (FITC; 1:250, Sigma) or tetramethyl rhodamine iso-thiocyanate (TRITC; 1:250, Sigma).

2.10 STATISTICAL ANALYSIS

Quantitative analysis was performed using GraphPad Prism 4.0 software (GraphPad Software, San Diego, CA). Results are expressed as mean and standard error of the

mean with a minimum n of 3. Each n value represents data from each animal. One way analysis of variance (ANOVA) followed by Tukey post-tests were performed while comparing three or more groups of the same genotype, differing in treatment. Two-way Analysis of Variance (ANOVA) followed by Bonferroni post hoc tests were performed when groups varied in terms of treatment as well as genotype. An unpaired two-tailed t-test was used to compare between two groups of the same genotype.

CHAPTER 3: RESULTS

3.1 *Mist1*$^{-/-}$ mice on the Lieber-DeCarli ethanol diet have no overt phenotype

The effects of chronically feeding mice an ethanol-supplemented liquid Lieber-DeCarli (LDC) diet, which contains 36% kcal from ethanol were examined. As a control, animals were placed on an identical diet with the calories from ethanol being replaced by carbohydrates. However, this diet contained a significant amount of calories from fat (36%). Therefore, mice maintained on regular breeder's chow were also included as controls. See Table 2.1 for constituents of each diet. The breeder's chow (denoted BC) contained 22% of kcal from fat.

To determine if the diets were affecting overall health, mice were initially weighed daily and then weekly and monitored for any signs of distress (grooming, excessive weight loss, food consumption, pilliated hair). Throughout the study, the average weight of the *Mist1*$^{-/-}$ cohort of animals was less than diet-matched WT mice, although the difference did not reach statistical significance. WT and *Mist1*$^{-/-}$ mice on the LDC-E and LDC-C diets consumed equivalent kcal amounts throughout the length of the study, with minimal individual variability in daily caloric intake (**Figure 3.1A**). Even with similar kcal consumption, the rate of weight gain was significantly higher in LDC-C fed mice for both genotypes compared to LDC-E counterparts (WT- $P<0.001$, n=11 (LDC-C), n=12 (LDC-E); *Mist1*$^{-/-}$- $P<0.05$, n=11 (LDC-C), n=12 (LDC-E)) or breeder chow fed mice (WT- $P<0.001$, n=7; *Mist1*$^{-/-}$- $P<0.01$, n=7) (**Figure 3.1B**), suggesting that any weight gain was due to the fat in the diet and that ethanol offset this effect. Observations from studies in

the literature indicate that ethanol itself has no effect on weight gain in rats or mice (Pandol et al, 1999; Perides et al, 2005), supporting the findings in this thesis. Interestingly, WT mice on the LDC-C diet gained significantly more weight than *Mist1*$^{-/-}$ mice ($P<0.01$).

To assess pancreatic damage, typical parameters of pancreatitis, including elevated serum amylase levels and pancreatic edema were compared at time of sacrifice. Analysis of serum amylase levels (**Figure 3.2A**) and pancreatic edema (**Figure 3.2B**) revealed that the LDC-E diet had no significant effect compared to the LDC-C diet.

Figure 3.1. WT and *Mist1*$^{-/-}$ mice show no overt response to ethanol feeding. Caloric intake **(A)** and weight gain **(B)** was monitored over six weeks of feeding with a Lieber-DeCarli Ethanol (LDC-E), LDC high fat (LDC-C) or breeder's chow (BC) diet. Letters represent statistically significant differences between groups. LDC-C fed mice gained significantly more weight than LDC-E mice (WT- $P<0.001$, n=11 (LDC-C), n=12 (LDC-E); *Mist1*$^{-/-}$- $P<0.05$, n=11 (LDC-C), n=12 (LDC-E)) as wells as BC fed mice (WT- $P<0.001$, n=7; *Mist1*$^{-/-}$- $P<0.01$, n=7). Groups were compared using a two-way ANOVA and a Bonferroni post-hoc test: n=7 (BC), n=11 (LDC-C), n=12 (LDC-E). The LDC-C diet resulted in increased weight gain in both genotypes.

A

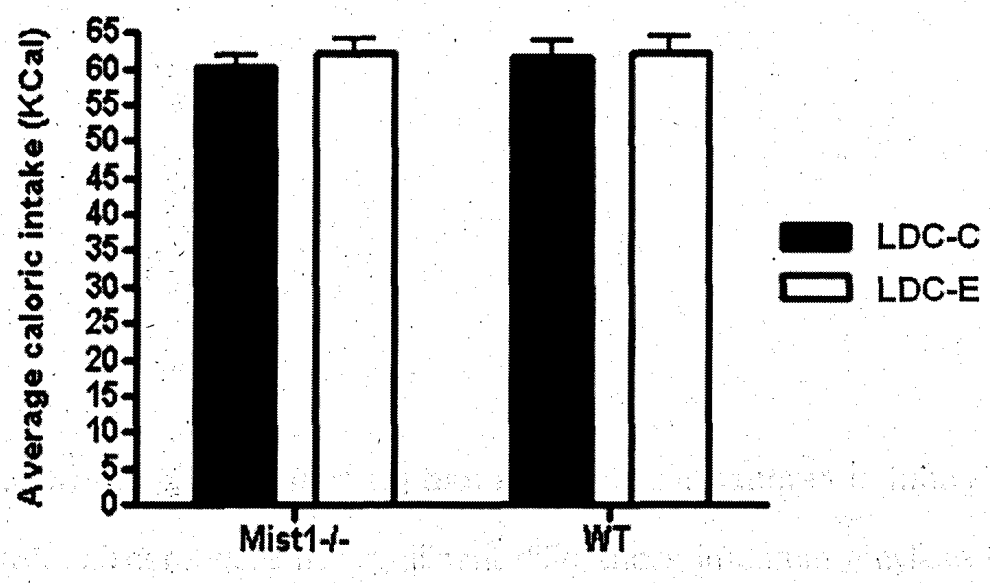
Average caloric intake (KCal)
65
60
55
50
45
40
35
30
25
20
15
10
5
0
Mist1-/-
WT
LDC-C
LDC-E

B

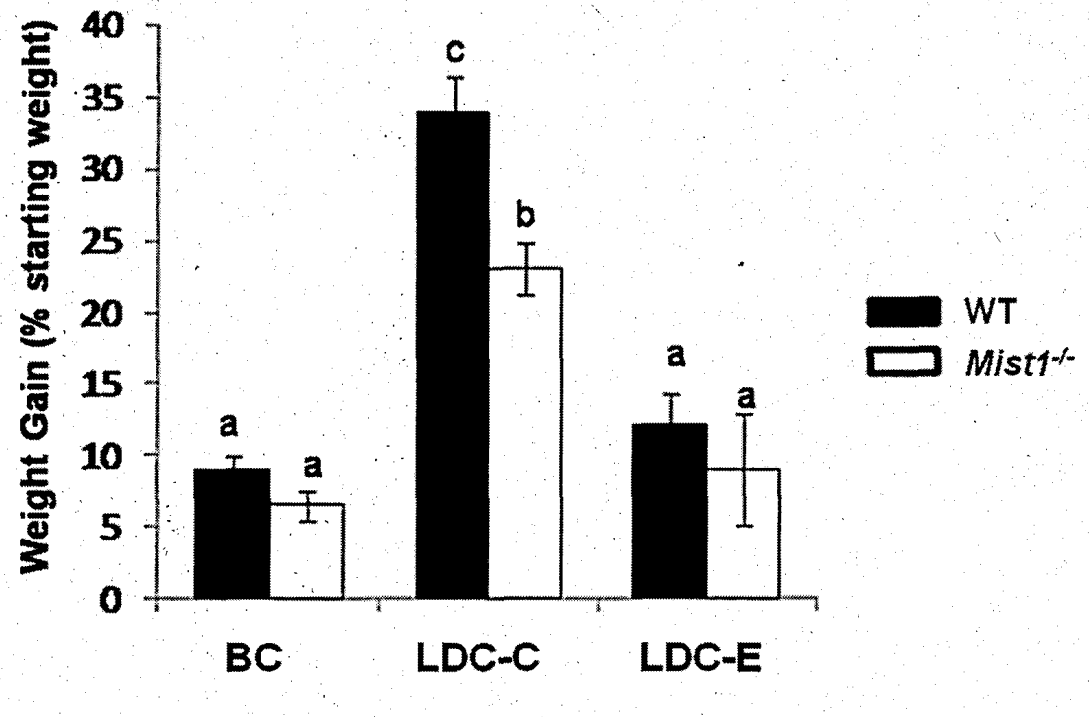
Weight Gain (% starting weight)
40
35
30
25
20
15
10
5
0
a
a
c
b
a
a
BC
LDC-C
LDC-E
WT
Mist1-/-

Figure 3.2.Chronic ethanol feeding has no effect on pancreatic injury parameters in *Mist1*$^{-/-}$ mice. There were no significant differences in serum amylase levels (**A**) or pancreatic edema (**B**) between *Mist1*$^{-/-}$and WT mice on the LDC-E or LDC-C diets. Groups were compared using a two way ANOVA and a Bonferroni post-hoc test: P=0.5645 (serum amylase); P= 0.2469 (edema). n=11 (LDC-C), n=12 (LDC-E).

A

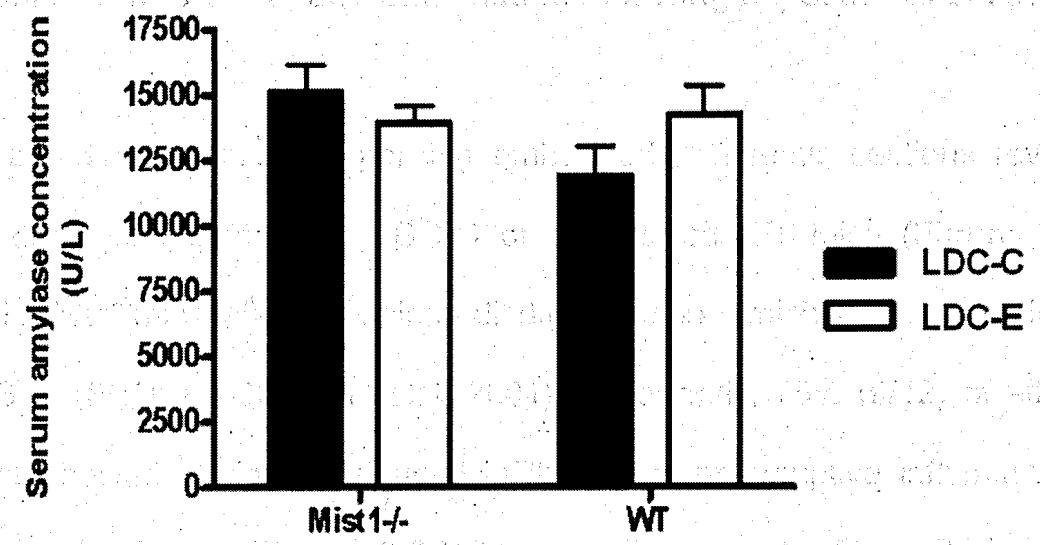
Serum amylase concentration (U/L)
17500
15000
12500
10000
7500
5000
2500
0
Mist1-/-
WT
LDC-C
LDC-E

B

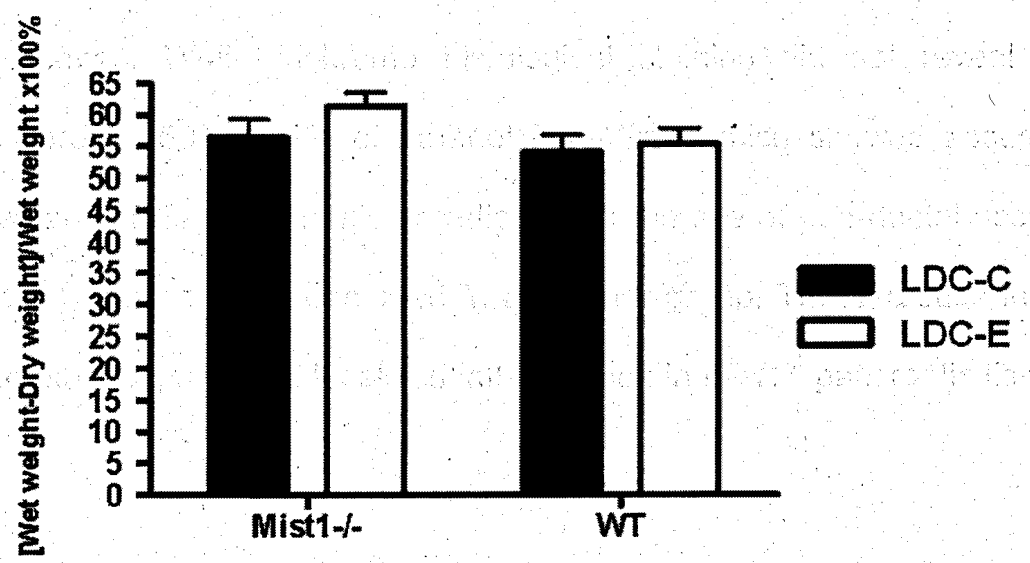
[Wet weight-Dry weight]/Wet weight x100%
65
60
55
50
45
40
35
30
25
20
15
10
5
0
Mist1-/-
WT
LDC-C
LDC-E

3.2 Histological analysis of pancreatic tissue following exposure to ethanol

Trichrome and H&E staining of paraffin embedded pancreatic sections revealed no signs of pathological damage in LDC-C or LDC-E fed WT mice (**Figure 3.3A, B**). Control fed *Mist1*$^{-/-}$mice showed acinar disorganization, which is a hallmark of mice lacking MIST1 (**Figure 3.3C**; Pin et al, 2001). Importantly, 75% (9/12) of ethanol fed *Mist1*$^{-/-}$ mice showed obvious periductal infiltration of presumptive inflammatory cells within pancreatic tissue (**Figure 3.3D**). Immunofluorescent (IF) analysis of frozen pancreatic sections for the T-lymphocyte marker CD4 confirmed these cells to be lymphocytes (**Figure 3.3E, F**). Interestingly, IF analysis also revealed smaller accumulations of CD4 positive cells in all other LDC-E fed *Mist1*$^{-/-}$ pancreatic tissue that were not evident in H&E stained tissue (**Figure 3.3E, F**). Similar staining of WT and non LDC-E groups showed no such CD4 positive cells within the pancreatic interstitium (data not shown). While trichrome histological staining did not reveal significant pancreatic fibrosis, 50% (6/12) of ethanol fed *Mist1*$^{-/-}$ mice showed accumulation of presumptive adipocytes, often located adjacent to the site of peri-ductal accumulations (**Figure 3.3Di**) that were not observed in any other group. These results indicate that exposure to ethanol promoted localized inflammation in *Mist1*$^{-/-}$ pancreatic tissue.

Figure 3.3. *Mist1*$^{-/-}$ pancreata develop periductal accumulations of inflammatory cells in response to ethanol feeding. Representative photomicrographs of Gomori's trichrome stained pancreatic sections from WT **(A, B)** and *Mist1*$^{-/-}$ mice **(C, D)** fed a LDC-C **(A, C)** or LDC-E **(B, D)** diet for 6 weeks. Higher magnification images **(Ai-Di)** were used to highlight specific morphological events. Cellular accumulations (arrowhead) surrounding ducts (*) and adipose accumulations (arrow) were observed only in LDC-E fed *Mist1*$^{-/-}$ mice. **(E, F)** IF analysis for the T-lymphocyte marker CD4 **(E)** indicated that these accumulations consisted of lymphocytes and that lymphocyte infiltration occurred in 75% of LDC-E *Mist1*$^{-/-}$ mice (9/12). Sections were co-stained with DAPI **(F)** to reveal all cells. Magnification bars= 40 μm.

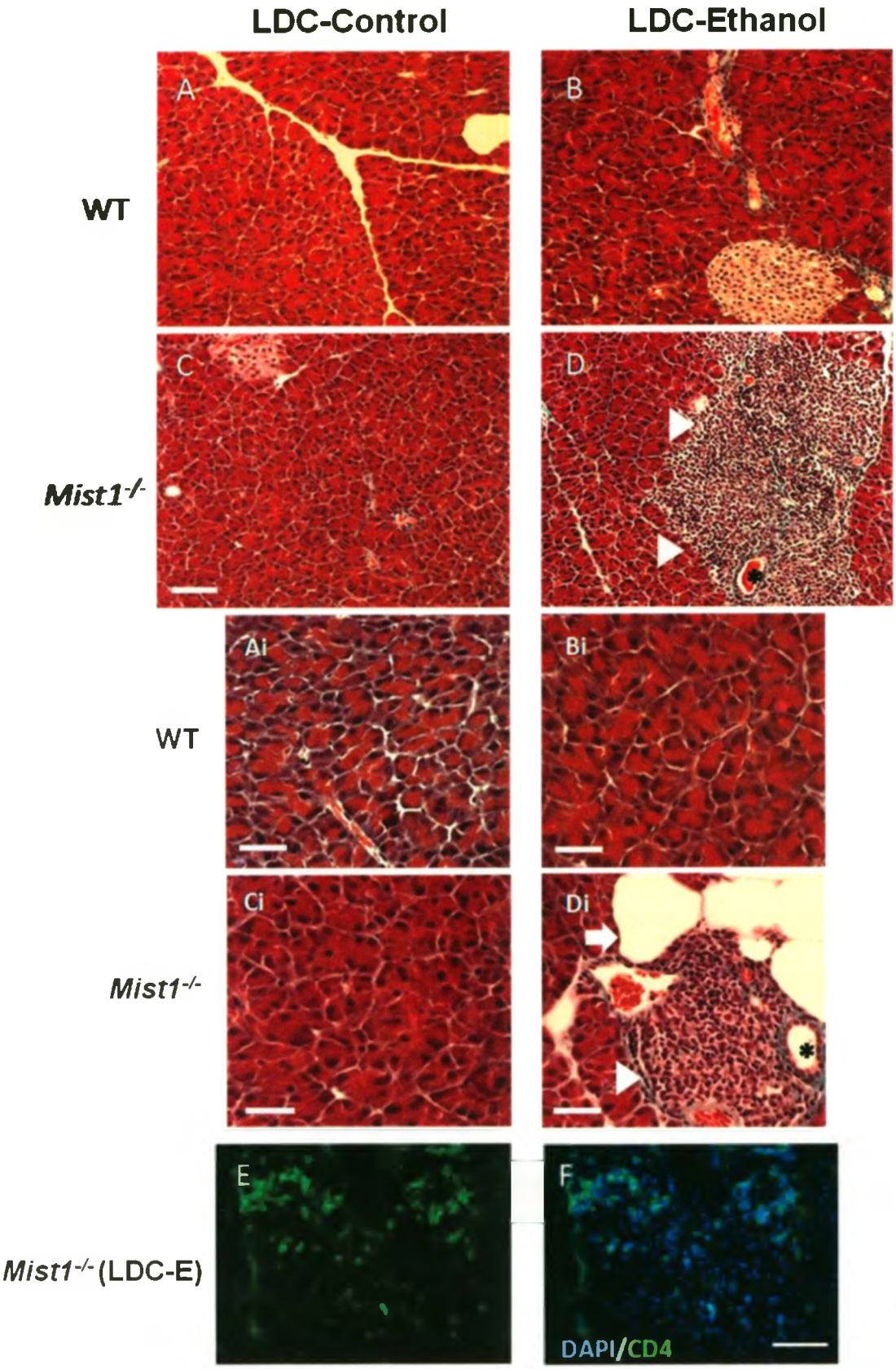
LDC-Control
LDC-Ethanol
WT
A
B
Mist1-/-
C
D
WT
Ai
Bi
Mist1-/-
Ci
Di
Mist1-/- (LDC-E)
E
F
DAPI/CD4

3.3 Effects of chronic ethanol feeding on the UPR in pancreatic acinar cells

Recent reports have shown that chronic ethanol exposure leads to increased accumulation of *sXbp1* in mouse pancreatic acinar cells (Lugea et al, 2011). *Xbp1*$^{+/-}$ mice show increased inflammation and pancreatic injury upon ethanol exposure, suggesting the UPR acts in a protective fashion to prevent ethanol-induced damage (Lugea et al, 2011). Therefore, activation of the three arms of the UPR (peIF2α activity as an indicator of activation of the PERK pathway, BiP/GRP78 expression as one output of the ATF6 pathway and splicing of *Xbp1* mRNA to indicate IRE1 activation) was examined in response to adverse diets.

RT-PCR analysis revealed increased splicing of *Xbp1* (**Figure 3.4 A, B**) in response to LDC-E feeding in WT acinar cells. Surprisingly, there is an increase in the ratio of *sXbp1/uXbp1* in LDC-C fed mice as well, indicating that a diet high in fat also activates the IRE1 pathway of the UPR (**Figure 3.4 A, B**). Both diets also lead to an increase in the total levels of *Xbp1* mRNA, suggesting increased activity of ATF6. Immunoblot (IB) analysis showed similar increases in peIF2α (**Figure 3.4C, D**) in response to LDC-C and LDC-E feeding, relative to breeder chow fed controls, indicating activation of the PERK signaling pathway. However, IB analysis revealed no change in BiP/GRP78 expression (**Figure 3.4 C, E**) another target of ATF6 (Wang et al, 2000). In summary, the PERK and IRE1 arms of the UPR were activated in pancreatic acinar cells in response to chronic high-fat and ethanol diets.

Figure 3.4. Chronic ethanol exposure activates the PERK and IRE1 arms of the UPR in pancreatic acinar cells. (**A**) RT-PCR analysis of *Xbp1* splicing in mice fed breeder chow (BC), LDC-E or LDC-C diets revealed increased splicing of *Xbp1* mRNA in response to both LDC-E and LDC-C diets only in WT pancreatic tissue. (**B**) Quantification of the ratio of spliced (*s*) *Xbp1* to unspliced (*u*) *Xbp1* as determined by densitometric analysis of images in A. (**C**) Immunoblot analysis of peIF2α and BiP/GRP78 expression, as an indicator of activation of the PERK and ATF6 pathways of the UPR respectively, in mice fed either breeder chow (BC), LDC-E or LDC-C diets. (**D**) Quantitative analysis of peIF2α normalized to β-Actin. (**E**) Quantitative analysis of BiP/GRP78 normalized to β-actin. Each lane represents data from individual mice. Groups were compared using a one-way ANOVA and a Tukey's post-hoc test: *P < 0.05, **P< 0.01. n=3 (BC), n=6 (LDC-C & E).

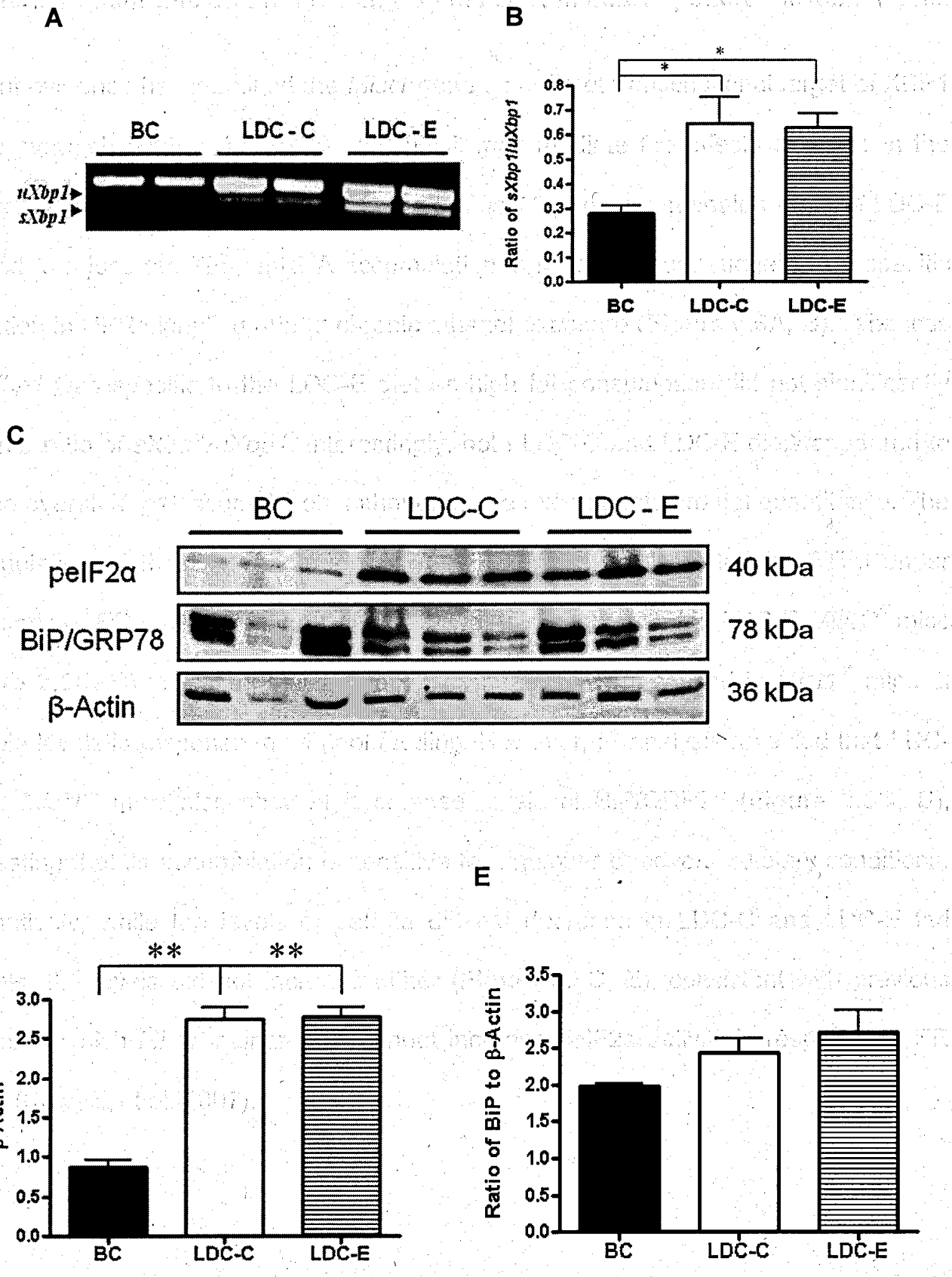
A
BC
LDC - C
LDC - E
uXbp1
sXbp1
B
Ratio of sXbp1/uXbp1
BC
LDC-C
LDC-E
C
BC
LDC-C
LDC - E
peIF2α
BiP/GRP78
β-Actin
40 kDa
78 kDa
36 kDa
D
Ratio of peIF2α to β-Actin
BC
LDC-C
LDC-E
E
Ratio of BiP to β-Actin
BC
LDC-C
LDC-E

3.4 Effects of chronic ethanol feeding on the UPR in *Mist1*$^{-/-}$ pancreatic acinar cells

Recent evidence has identified the *Mist1* gene as a direct transcriptional target of XBP1 in the stomach (Huh et al, 2010) and that it may mediate the effects of XBP1 in the pancreas (Hess et al, 2011). Examination of *Mist1*$^{-/-}$ pancreas revealed that the LDC-E diet led to a loss of *sXbp1* mRNA accumulation in *Mist1*$^{-/-}$ tissue, suggesting a specific alteration in UPR signaling due to chronic ethanol exposure (**Figure 3.5A, B**). The loss of *sXbp1* was specific to the LDC-E diet as high fat consumption did not significantly alter the ratio of *sXbp1/uXbp1*. Interestingly, both LDC-C and LDC-E diets appeared to reduce overall *Xbp1* accumulation, although these experiments are not quantitative. The accumulation of the ER chaperone BiP/GRP78, which is regulated by ATF6 under conditions of ER stress (Wang et al, 2000) was also decreased in LDC-E *Mist1*$^{-/-}$ mice (**Figure 3.5C, D**) indicating that activation of the UPR was reduced in *Mist1*$^{-/-}$ mice at multiple levels in response to ethanol feeding. However, IB analysis revealed that LDC-C fed *Mist1*$^{-/-}$ mice also showed decreased levels of BiP/GRP78 (**Figure 3.5C, D**), suggesting that its accumulation is sensitive to a number of adverse dietary conditions. Alternatively, while the levels of peIF2a did not decrease in LDC-C and LDC-E fed animals, the levels did not increase either (**Figure 3.5C, E**), consistent with previous studies in which *Mist1*$^{-/-}$acinar cells cannot increase peIF2a activity in response to ER stress (Kowalik et al, 2007).

Figure 3.5. Chronic ethanol exposure attenuates the PERK and IRE1 arms of the UPR in *Mist1*$^{-/-}$ pancreatic acinar cells. (**A**) RT-PCR analysis of *Xbp1* splicing in *Mist1*$^{-/-}$ mice fed breeder chow (BC), LDC-E or LDC-C diets revealed decreased splicing of *Xbp1* mRNA in response to the LDC-E alone. (**B**) Quantification of the ratio of spliced (*s*) *Xbp1* to unspliced (*u*) *Xbp1* as determined by densitometric analysis of images in A. (**C**) Immunoblot analysis of peIF2α and BiP/GRP78 expression, as an indicator of activation of the PERK and ATF6 pathways of the UPR respectively, in mice fed either breeder chow (BC), LDC-E or LDC-C diets. (**D**) Quantitative analysis of peIF2α normalized to β-actin. (**E**) Quantitative analysis of BiP/GRP78 normalized to β-actin. Each lane represents data from individual mice. Groups were compared using a one-way ANOVA and a Tukey's post-hoc test: *P < 0.05, **P< 0.01. n=3 (BC), n=6 (LDC-C & E).

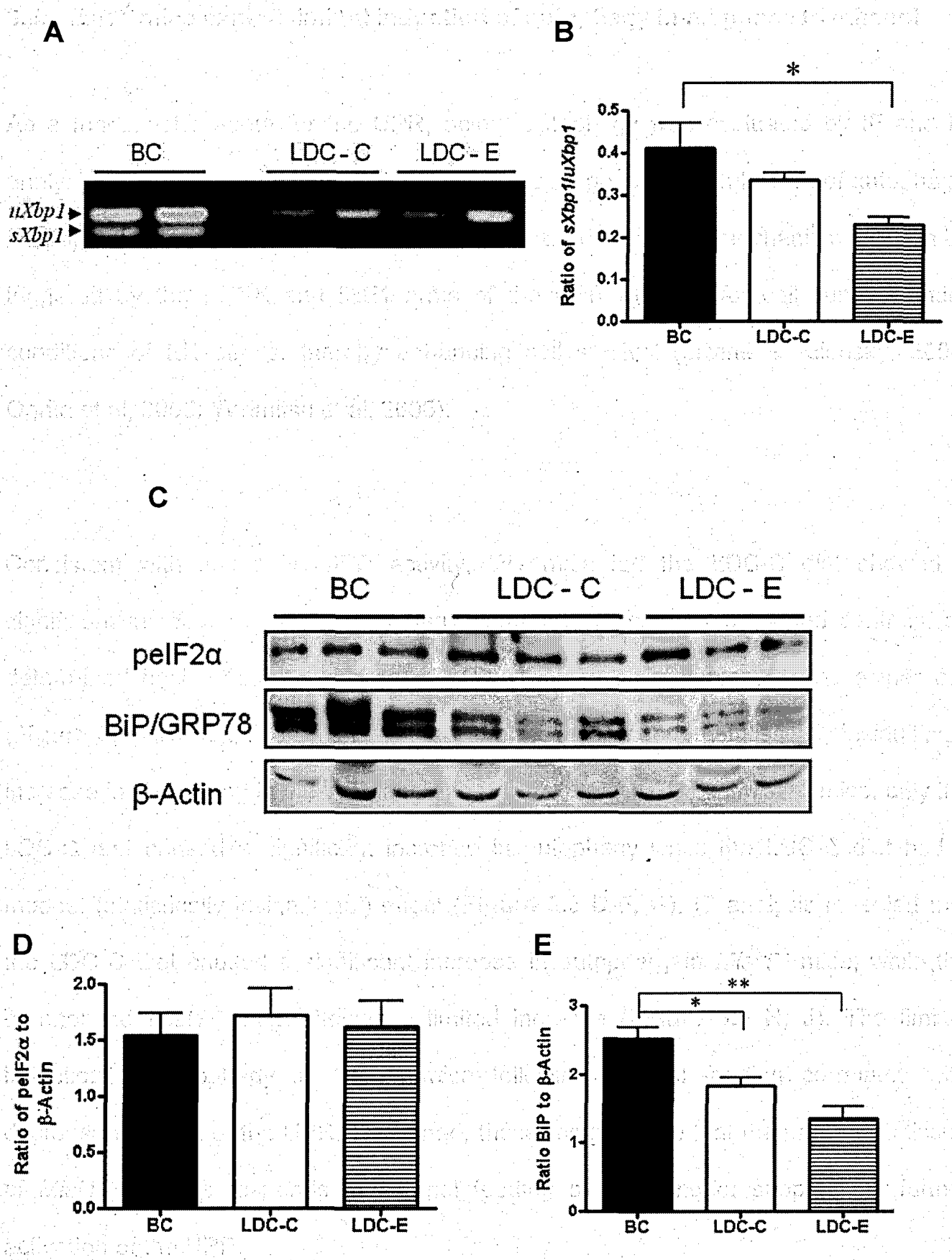
A
BC
LDC - C
LDC - E
uXbp1
sXbp1
B
*
Ratio of sXbp1/uXbp1
0.5
0.4
0.3
0.2
0.1
0.0
BC
LDC-C
LDC-E
C
BC
LDC - C
LDC - E
peIF2α
BiP/GRP78
β-Actin
D
Ratio of peIF2α to β-Actin
2.0
1.5
1.0
0.5
0.0
BC
LDC-C
LDC-E
E
**
*
Ratio BIP to β-Actin
3
2
1
0
BC
LDC-C
LDC-E

3.5. *Mist1*$^{-/-}$ mice exhibit limited induction of autophagy in response to ethanol

As a functional readout for the UPR, acinar autophagy was evaluated by IF and IB analysis of LC3-II, a protein associated with autophagosomal membranes of autophagic vacuoles (Levine & Klionsky, 2004). Autophagy is a degradation mechanism that can be triggered by the PERK and IRE1 arms of the UPR to allow for cell survival under conditions of ER stress, thereby enhancing cell survival (Levine & Klionsky, 2004; Ogata et al, 2006; Yorimitsu et al, 2006).

Consistent with increased UPR activity, WT mice fed the LDC-C diet showed a significant increase in acinar autophagy compared to breeder chow fed controls, as determined by IF analysis of area of LC3-II puncta as a percent of the acinar cell (**Figure 3.6 A-C, G**). The LDC-E diet led to a modest, although statistically insignificant increase in autophagy in the WT pancreas (**Figure 3.6 A-C, G**). In *Mist1*$^{-/-}$ mice, only the LDC-C diet caused a significant increase in autophagy while the LDC-E diet had a modest (statistically insignificant) effect (**Figure 3.6 D-F, G**). IB analysis revealed that the LDC-C diet caused a significant increase in autophagy in *Mist1*$^{-/-}$ mice, while the ethanol fed *Mist1*$^{-/-}$ mice showed a limited increase (**Figure 3.6 H, J**). The limited induction of autophagy in *Mist1*$^{-/-}$ mice following ethanol feeding correlates with decreased activity of the UPR. Combined, these results show that the pancreatic tissue of *Mist1*$^{-/-}$ animals responds to ethanol feeding by reducing or suppressing further activation of the UPR.

Figure 3.6. Ethanol-fed *Mist1*$^{-/-}$ mice show limited increases in autophagy. Representative photomicrographs of pancreatic tissue sections from WT and *Mist1*$^{-/-}$ mice fed either breeder chow (A,D), LDC-C (B,E) or LDC-E (C,F) diet and stained for the autophagy marker, LC3II (punctate staining in red). Dapi (blue) was used to counterstain nuclei. (**G**) Quantitative analysis of LC3II puncta, shown as the area of LC3 dots per area of DAPI stained nuclei. Groups were compared using One-way ANOVA and a Tukey post- hoc test: *P<0.05. n=3 (BC), n=5 (LDC-C & LDC-E). Magnification bar = 20 μm. (**H**) Immunoblot analysis of LC3 lipidation in WT and *Mist1*$^{-/-}$ mice fed either breeder chow, LDC-C or LDC-E diets. (**I**) Quantitative analysis of the ratio of LC3II to LC3I in WT mice.(**J**) Quantitative analysis of the ratio of LC3II to LC3I in *Mist1*$^{-/-}$ mice. Groups were compared using a one-way ANOVA and a Tukey's post- hoc test: Each lane represents data from individual mice. *P<0.05 **P<0.01. n=3 (BC), n=6 (LDC-C & LDC-E).

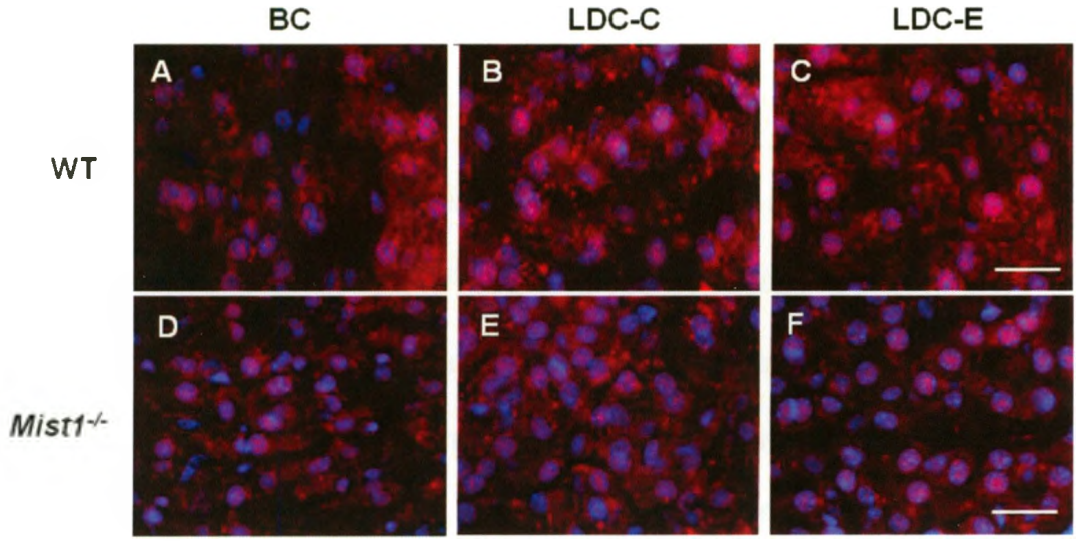
BC
LDC-C
LDC-E
A
B
C
WT
D
E
F
Mist1-/-

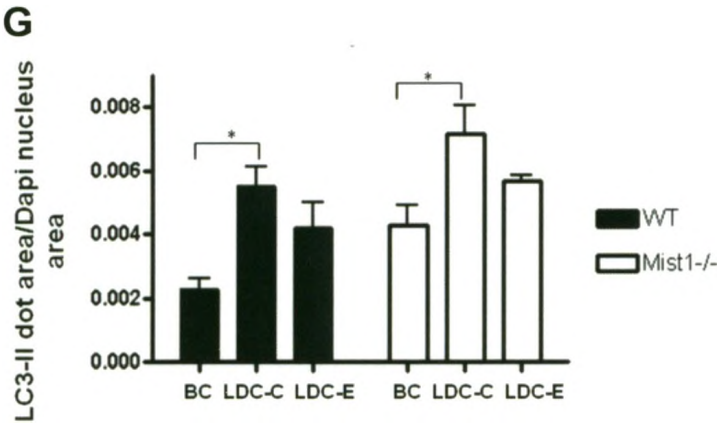
G
LC3-II dot area/Dapi nucleus area
0.008
0.006
0.004
0.002
0.000
*
*
BC LDC-C LDC-E BC LDC-C LDC-E
WT
Mist1-/-


H
WT
Mist1-/-
BC
LDC-C
LDC-E
BC
LDC-C
LDC-E
LC3I
LC3II

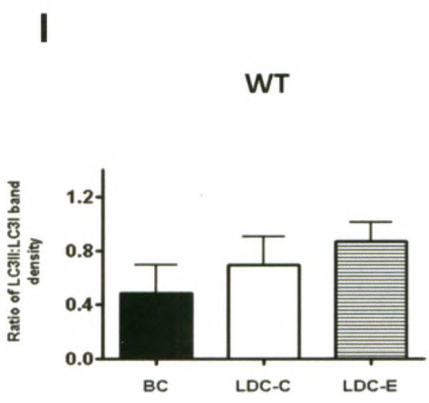
I
WT
Ratio of LC3II:LC3I band density
1.2
0.8
0.4
0.0
BC
LDC-C
LDC-E

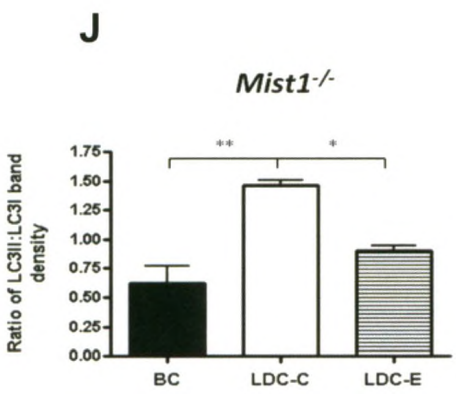
J
Mist1-/-
Ratio of LC3II:LC3I band density
1.75
1.50
1.25
1.00
0.75
0.50
0.25
0.00
**
*
BC
LDC-C
LDC-E

3.6 UPR in the *Mist1*$^{-/-}$ pancreas

The data so far suggests that *Mist1*$^{-/-}$ mice failed to activate the UPR in response to adverse dietary conditions. RT-PCR analysis of *Xbp1* splicing in WT and *Mist1*$^{-/-}$ pancreas in response to ethanol indicated that the breeder chow fed *Mist1*$^{-/-}$ tissue had increased levels of *sXbp1* compared to WT counterparts (**Figures 3.4 A, B & 3.5 A, B**). Hence, activation of UPR mediators including BiP/GRP78, GADD34, XBP1 and peIF2α was assessed in 2 and 6 month old *Mist1*$^{-/-}$ and WT mice by IB analysis.

At 2 months of age, protein levels of BiP/GRP78, GADD34 and sXBP1 were significantly increased in pancreatic tissue of breeder chow fed *Mist1*$^{-/-}$ mice compared to age-matched WT mice (**Figure 3.7A, C-E**) indicating that the *Mist1*$^{-/-}$ tissue is under stress . Protein levels of peIF2α remained unchanged. This can be explained by the fact that GADD34 is a negative regulator of eIF2α phosphorylation, and chronically elevated levels of GADD34 will prevent an increase in eIF2α phosphorylation (Connor et al, 2001). In contrast, at 6 months of age, no significant differences were observed in BiP/GRP78 and sXBP1 expression between WT and *Mist1*$^{-/-}$ pancreatic tissue, while increased GADD34 expression in the *Mist1*$^{-/-}$ pancreas was maintained (**Figure 3.7B**). peIF2α levels also remained unchanged at 6 months of age in *Mist1*$^{-/-}$ pancreatic tissue. These results suggest that the *Mist1*$^{-/-}$ pancreas is chronically stressed and the loss of UPR activation between 2 and 6 months of age rendered the tissue increasingly susceptible to environmental stressors such as an ethanol laced diet.

Figure 3.7. *Mist1*$^{-/-}$ pancreas show age-related changes in UPR activation. Immunoblot analysis of key unfolded protein response markers in 2 (**A**) and 6-month old (**B**) WT and *Mist1*$^{-/-}$ whole pancreatic lysates from 2-month old *Mist1*$^{-/-}$ mice showed significant increases in the expression of BiP/GRP78 (P=<0.001) (**C**), GADD34 (P<0.01) (**D**) and sXBP1 (P<0.01) (**E**) but not in peIF2α (P=0.743) or uXBP1 (P= 0.532). There were no significant differences in expression of any of the afore-mentioned markers between 6-month old WT and *Mist1*$^{-/-}$ mice. (**C**) Quantitative analysis comparing BiP/GRP78 (**C**), GADD34 (**D**) and sXBP1 (**E**) accumulation at 2 months in WT and *Mist1*$^{-/-}$ mice. Total eIF2α served as a normalization control. Groups were compared using a Student's T-test: *p <0.05. n=3.

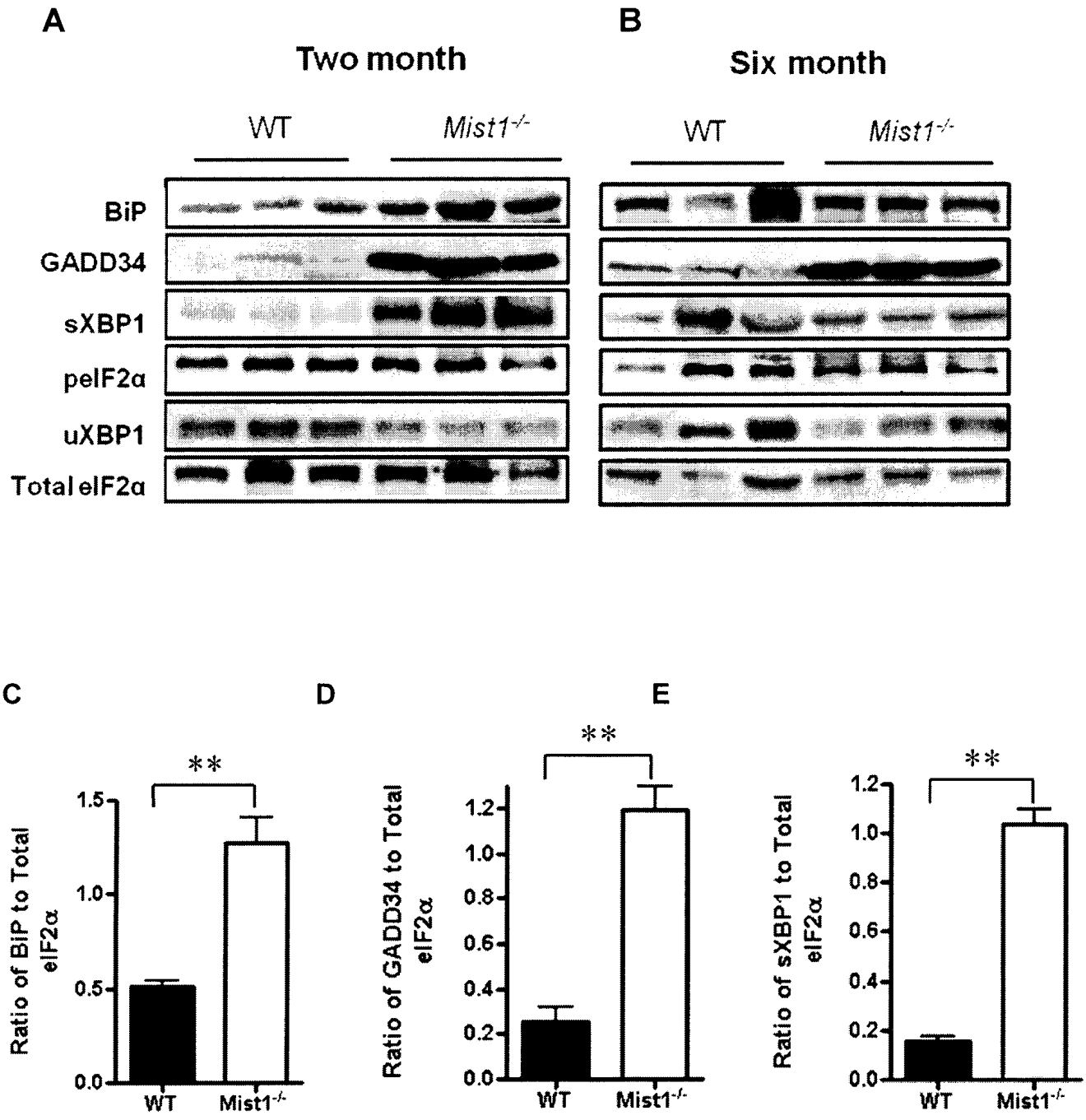
A
Two month
WT
Mist1-/-
BiP
GADD34
sXBP1
peIF2α
uXBP1
Total eIF2α
B
Six month
WT
Mist1-/-
C
Ratio of BiP to Total eIF2α
**
1.5
1.0
0.5
0.0
WT
Mist1-/-
D
Ratio of GADD34 to Total eIF2α
**
1.2
1.0
0.8
0.6
0.4
0.2
0.0
WT
Mist1-/-
E
Ratio of sXBP1 to Total eIF2α
**
1.2
1.0
0.8
0.6
0.4
0.2
0.0
WT
Mist1-/-

3.7 Chronic ethanol exposure followed by cerulein-induced acute pancreatitis

Mist1$^{-/-}$ tissue displays a limited or decreased UPR response to acute and chronic stress. If adaptation to chronic activation of the UPR observed in *Mist1*$^{-/-}$ pancreata was responsible for the inability to further enhance activity of the pathway when an additional stress is introduced, then the ability of LDC-E and LDC-C fed wild types to activate the UPR in response to acute stress should be compromised. To test this hypothesis, the pancreatic response of 3-4 month old diet challenged WT mice to CIP was examined. Pancreatitis was initiated through four hourly injections of cerulein in LDC-E, LDC-C and breeding chow fed mice. This produced a UPR response including increased activity of pPERK and its downstream targets, peIF2α, ATF3 and ATF4. The activity of the UPR mediators was assessed four hours after initiation of CIP. Parameters of acute pancreatitis such as serum amylase levels and pancreatic edema were also assessed at the 4 hour time-point.

Analysis of serum amylase levels revealed a significant decrease in response to the LDC-C diet compared to breeder chow fed controls (**Figure 3.8 A**). This finding is in contrast to findings in the literature (Deng et al, 2004; Ye et al, 2010) where initiation of CIP in high fat diet and ethanol fed WT mice caused significant increases in blood amylase and lipase levels compared to regular diet fed mice.

IB analysis of key UPR markers including BiP, peIF2α, ATF3 and ATF4 revealed no differences between different treatments (**Figure 3.9 A**). Interestingly, both LDC-C and

LDC-E diets led to a significant increase in pPERK activity (**Figure 3.9 A, B**). This was surprising, given that downstream targets of pPERK (such as peIF2α, ATF3 and ATF4) remained unaffected by chronic ethanol or high fat diets upon induction of acute pancreatitis.

Figure 3.8. Chronic ethanol exposure followed by an acute pancreatitis episode (4 hour cerulein-induced pancreatitis) had no effect on serum amylase levels in WT mice, while chronic feeding of a the LDC-C diet led to a significant decrease in serum amylase levels compared to breeder c how fed mice. Groups were compared using a one-Way ANOVA and a Tukey's post-hoc test: *$P<0.05$. n=4.

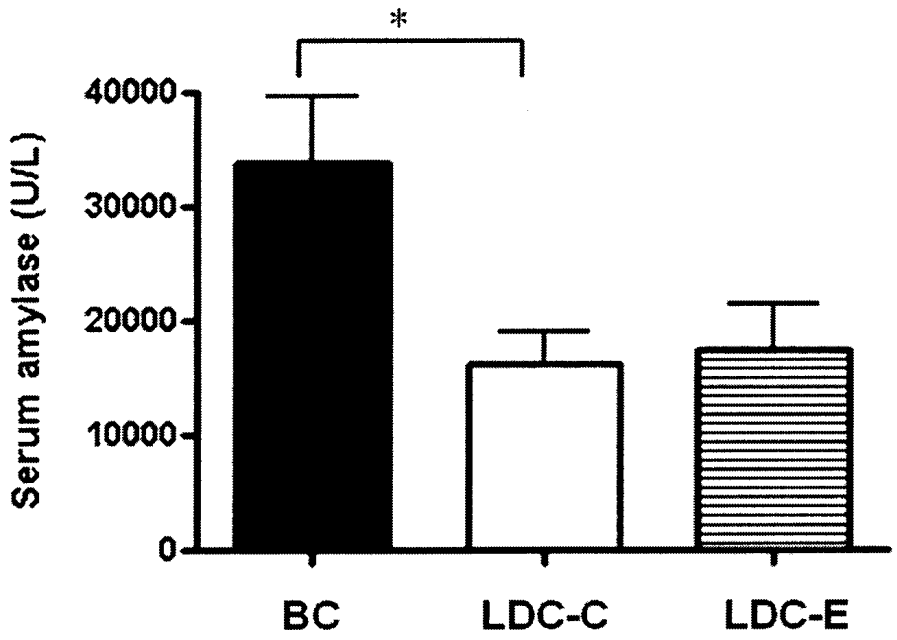
*
40000
30000
20000
10000
0
Serum amylase (U/L)
BC
LDC-C
LDC-E

Figure 3.9. Chronic ethanol exposure followed by initiation of acute pancreatic injury has no additional effect on the UPR in pancreatic acinar cells. (A) Immunoblot analysis of UPR markers pPERK, peIF2α, ATF3, ATF4 and BiP in mice fed either a breeder chow (BC) diet, LDC-E or LDC-C diet for 6 weeks, followed by initiation of acute pancreatitis by four hourly injections of cerulein. There were no significant differences in UPR mediators such as peIF2α (P=0.562), ATF3 (P=0.413), ATF4 (P= 0.563) and BiP (P=0.201). β-Actin served as a loading control. **(B)** Quantitative analysis of pPERK activation. Groups were compared using a one way ANOVA and a Tukey's post-hoc test: ***P<0.001. n= 4.

A

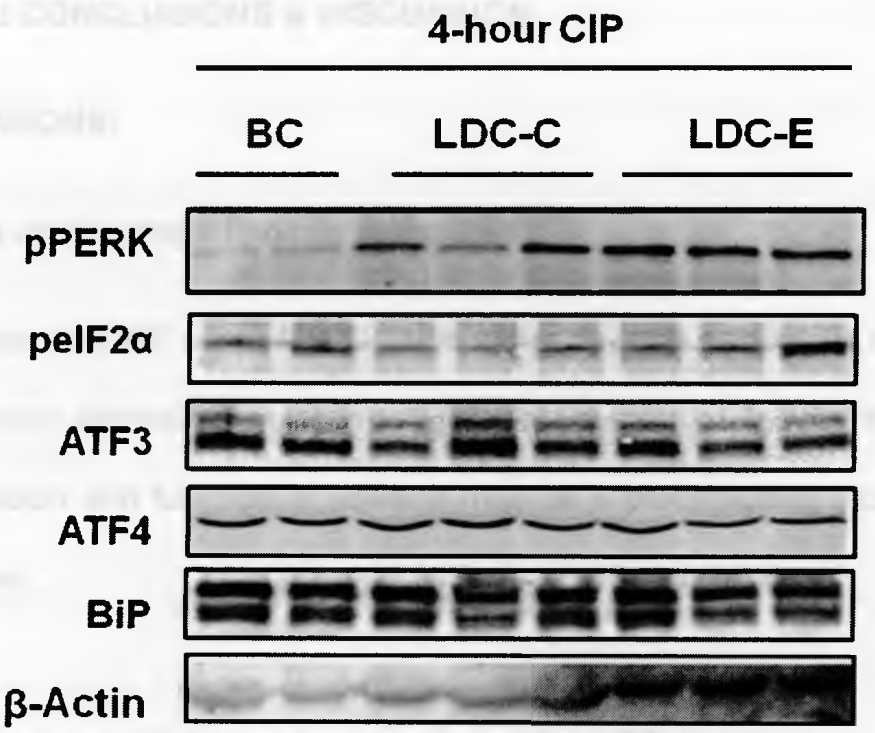
4-hour CIP
BC
LDC-C
LDC-E
pPERK
peIF2α
ATF3
ATF4
BiP
β-Actin

B

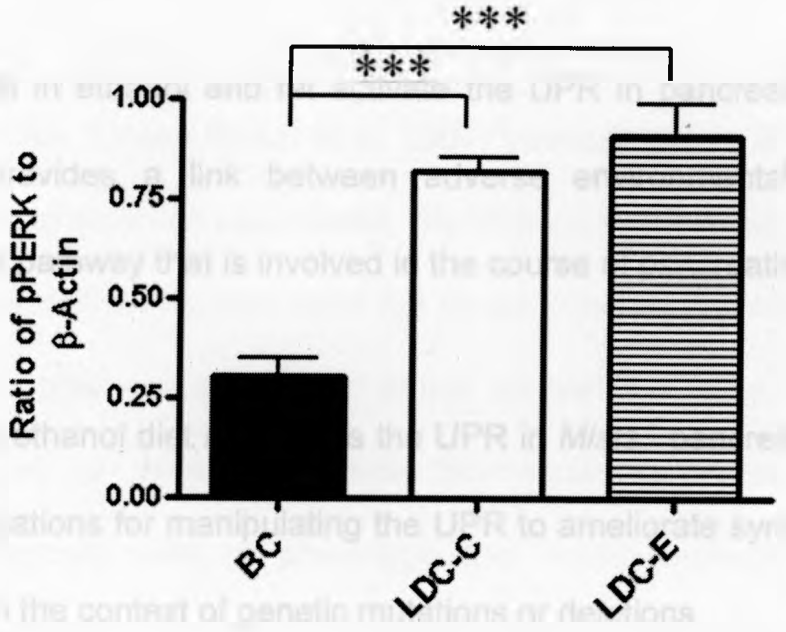
***
***
1.00
0.75
0.50
0.25
0.00
Ratio of pPERK to β-Actin
BC
LDC-C
LDC-E

CHAPTER 4: CONCLUSIONS & DISCUSSION

4.1 CONCLUSIONS:

The following are the major findings in this thesis:

1. Compared to WT mice, *Mist1*$^{-/-}$ mice alone develop pancreatic injury in response to chronic ethanol consumption. This suggests that factors that affect MIST1 expression and function in humans may be a predisposing factor for pancreatic disease.

2. *Mist1*$^{-/-}$ mice exhibit chronic activation of the UPR that decreases over time. The loss of this protective cellular mechanism coincides with increased susceptibility to pancreatic injury.

3. Diets high in ethanol and fat activate the UPR in pancreatic acinar cells. This finding provides a link between adverse environmental conditions and a molecular pathway that is involved in the course of pancreatic disease.

4. A chronic ethanol diet attenuates the UPR in *Mist1*$^{-/-}$ pancreatic acinar cells. This has implications for manipulating the UPR to ameliorate symptoms of pancreatic disease in the context of genetic mutations or deletions.

5. Further enhancement of the UPR is prevented in WT mice exposed to chronic ethanol or high fat diets followed by an acute pancreatitis episode. This suggests that adverse dietary conditions may predispose individuals to pancreatitis due to lack of enhancement of the protective UPR.

4.2 DISCUSSION

Pancreatitis is a debilitating disease that targets the exocrine pancreas. While chronic alcohol abuse is a leading cause of pancreatitis in humans, animal models of alcoholic pancreatitis indicate that additional factors must be present to promote pancreatic injury associated with alcohol. The harmful effects of chronic alcohol exposure on the pancreas are well characterized. At the cellular level, ethanol sensitizes the pancreas by altering Ca^{2+} and NF-κB signaling, increases digestive and lysosomal enzyme content and leads to spatial alterations in SNARE-mediated regulated exocytosis (Cosen-Binker et al, 2007; Vonlaufen et al, 2007). Consistent with the current model of alcoholic pancreatitis, the findings in this thesis project indicate that a chronic ethanol diet on its own does not cause overt morphological damage to the pancreas. In the presence of chronic stress caused due to a lack of MIST1, the sensitizing effects of ethanol promote the accumulation of inflammatory and presumptive adipocyte cells, a phenotype that could represent a progression to pancreatitis. It remains to be seen if a longer duration of the ethanol diet results in the onset of the disease in these mice.

4.2.1 *Mist1*$^{-/-}$ mice are more sensitive to chronic ethanol consumption.

Mist1$^{-/-}$ mice develop periductal accumulations of inflammatory T cells in response to ethanol feeding that are not observed in congenic mice, suggesting that *Mist1*$^{-/-}$ mice are more sensitive to ethanol consumption in comparison to their WT counterparts. Furthermore, an absence of MIST1 function may be a link to increased susceptibility to environmental factors that promote pancreatic injury in humans.

The finding that absence of MIST1 enhances sensitivity to ethanol but not fat suggests the involvement of distinct molecular events in the pathogenesis of alcohol induced injury in these mice. What is the underlying cause of the development of inflammation in these animals? One possible target is the Ca^{2+} signalling pathway in acinar cells impacted by the production of toxic metabolites of ethanol and reactive oxygen species (ROS). Activation of ROS results in the generation of more ROS and subsequent deficits in the regulated exocytosis pathway (Gonzalez et al, 2006). Recent work also suggests that ethanol inhibits Ca^{2+} pump activity, preventing extrusion of Ca^{2+} from the cytosol (Fernández-Sánchez et al, 2009). These are believed to be some of the initiating events in ethanol mediated activation of pro-inflammatory factors during the course of ethanol induced pancreatitis (Pandol et al, 2003). Interestingly, *Mist1*$^{-/-}$ pancreatic acinar cells exhibit altered Ca^{2+} signalling, including a loss of Ca^{2+} oscillations and aberrant apical-basal Ca^{2+} waves following secretagogue stimulation (Luo et al, 2005) as well as decreased expression of modulators of cytoplasmic Ca^{2+}

including IP_3R and SPCA2 (Pin et al, 2001; Garside et al, 2010). It is likely that chronic ethanol feeding of *Mist1*$^{-/-}$ mice compounded the existing deficits in Ca^{2+} signalling, thereby initiating the onset of inflammation. It will be interesting to examine the in vitro effects of ethanol on isolated *Mist1*$^{-/-}$ acinar cells in the context of Ca^{2+} signalling and the activation of pro-inflammatory factors.

Another potential target is altered NF-κB signalling in ethanol-fed *Mist1*$^{-/-}$ mice. NF-κB is a transcription factor and a key mediator of the inflammatory pathway (Barnes and Karin, 1997). Gukovskaya et al (2002) have shown that ethanol's effects on NF-κB activation are dependent on its mode of metabolism in pancreatic acinar cells. Oxidative metabolites of ethanol, including acetaldehyde inhibited NF-κB activity while its non-oxidative metabolites, including FAEEs (fatty acid ethyl esters) activated NF-κB (Gukovskaya et al, 2002). While the relative contributions of the oxidative and non-oxidative metabolic pathways in pancreatic acinar cells are currently not well understood, alteration in NF-κB signalling is a key link to ethanol mediated inflammation. Examination of NF-κB activity in *Mist1*$^{-/-}$ mice before and after ethanol treatment will uncover potential alterations in this pathway and the resulting inflammation.

In addition to altered NF-κB signalling, ethanol has detrimental effects on the regulated exocytosis pathway in pancreatic acinar cells. An ethanol diet followed by post-prandial cholinergic stimulation leads to the displacement of SNARE (Soluble NSF Attachment Protein Receptor) proteins from zymogen granules, forming a complex with

their cognates on the basolateral acinar cell membrane and essentially re-directing exocytosis from the apical pole to the basolateral aspect of the cell (Cosen-Binker et al, 2007). This event has been identified as a key step in the early pathogenesis of pancreatitis as a consequence of elevated digestive enzyme levels in the interstitium (Watanabe et al, 1984). *Mist1*$^{-/-}$ mice show improper granule organization and disrupted exocytosis, one of several characteristics that make them more susceptible to secretagogue induced pancreatitis (Johnson et al, 2004; Kowalik et al, 2007). In the present study, elevated serum amylase levels were not observed due to ethanol feeding of the *Mist1*$^{-/-}$ mice and it is likely that the limited duration of exposure to the *Mist1*$^{-/-}$ pancreas or the age of the animals within this study - 2 to 4 months of age at the beginning of treatment – contribute to this mild phenotype.

Another likely cause for increased susceptibility of *Mist1*$^{-/-}$ mice to ethanol is differential activation of the UPR in response to stress. All three pathways of the UPR are activated in response to both L-arginine and cerulein-induced pancreatitis (Sans et al, 2003; Kubisch et al, 2006; Kowalik et al, 2007). Recently, the importance of XBP1, a key marker of the unfolded protein response (UPR), was examined in the context of ethanol-induced sensitivity to pancreatitis (Lugea et al, 2011). Chronic ethanol feeding of wild type (WT) mice led to increased activation of IRE1 (inositol requiring enzyme 1) and its target XBP1, and mice heterozygous for *Xbp1* (*Xbp1*$^{+/-}$) exhibited increased sensitivity to alcohol, based on the amount of acinar cell damage compared to WT mice

(Lugea et al, 2011). Collectively these studies suggest that events that alter the UPR may predispose individuals to ethanol-initiated pancreatitis.

4.2.2 *Mist1*$^{-/-}$ mice exhibit chronic activation of the UPR that changes over time.

Studies in our laboratory on 2 to 10-month old *Mist1*$^{-/-}$ mice revealed alterations in Ca^{2+} handling and accumulation of active digestive enzymes within the tissue similar to the initial events that occur during pancreatitis (Pin et al, 2001). These studies showed that the pancreatic disorganization observed in *Mist1*$^{-/-}$ mice was progressive, and that a subset of 10-month old mice developed pockets of acinar-ductal complexes, indicative of acinar to ductal trans-differentiation *in vivo*. However, only a subset (<10%) of these mice developed any type of inflammation or fibrosis characteristic of pancreatic injury, suggesting that protective mechanisms may be preventing development of the disease. A compelling candidate for this protective mechanism is the unfolded protein response (UPR). The UPR is believed to protect the tissue from significant injury in both experimental and ethanol induced models of pancreatic injury (Lugea et al, 2011). Indeed, compared to WT controls, *Mist1*$^{-/-}$ mice show extensive damage upon initiation of cerulein induced pancreatitis (CIP), coincident with an inability to fully activate the UPR (Kowalik et al, 2007). In the absence of additional stress, 2-month old *Mist1*$^{-/-}$ mice show elevated levels of sXBP1 and BiP/GRP78 while at 6 months of age, there is a return to WT levels of these proteins, suggesting an adaptive

(Lugea et al, 2011). Collectively these studies suggest that events that alter the UPR may predispose individuals to ethanol-initiated pancreatitis.

4.2.2 *Mist1*$^{-/-}$ mice exhibit chronic activation of the UPR that changes over time.

Studies in our laboratory on 2 to 10-month old *Mist1*$^{-/-}$ mice revealed alterations in Ca^{2+} handling and accumulation of active digestive enzymes within the tissue similar to the initial events that occur during pancreatitis (Pin et al, 2001). These studies showed that the pancreatic disorganization observed in *Mist1*$^{-/-}$ mice was progressive, and that a subset of 10-month old mice developed pockets of acinar-ductal complexes, indicative of acinar to ductal trans-differentiation *in vivo*. However, only a subset (<10%) of these mice developed any type of inflammation or fibrosis characteristic of pancreatic injury, suggesting that protective mechanisms may be preventing development of the disease. A compelling candidate for this protective mechanism is the unfolded protein response (UPR). The UPR is believed to protect the tissue from significant injury in both experimental and ethanol induced models of pancreatic injury (Lugea et al, 2011). Indeed, compared to WT controls, *Mist1*$^{-/-}$ mice show extensive damage upon initiation of cerulein induced pancreatitis (CIP), coincident with an inability to fully activate the UPR (Kowalik et al, 2007). In the absence of additional stress, 2-month old *Mist1*$^{-/-}$ mice show elevated levels of sXBP1 and BiP/GRP78 while at 6 months of age, there is a return to WT levels of these proteins, suggesting an adaptive

response over time. However, while this switch in UPR activity occurs relatively early, work from our lab has revealed that only the pancreas of aged *Mist1*$^{-/-}$ mice (12 and 18-month olds) contained periductal inflammatory infiltrate, positive for the T-lymphocyte marker, CD4 (Guinness and Pin, unpublished results). This suggests that while there is an adaptation in the UPR over time, its protective functions are intact in younger *Mist1*$^{-/-}$ mice. It is also likely that other protective pathways are playing a role in these mice..

What causes the switch in UPR activity between 2 and 6 months is currently unclear. It is possible that attenuating the UPR in response to chronic stress is protective to the tissue in the long run since continuous activation would impose translational attenuation that can be detrimental. This is consistent with the finding that GADD34 protein levels continue to be elevated in the *Mist1*$^{-/-}$ mice at all time points examined (2, 6 and 12 months). GADD34 works in a negative feedback fashion by promoting the dephosphorylation of peIF2α, thus inhibiting attenuation of protein translation brought upon by eIF2α phosphorylation (Connor et al, 2001). Therefore, chronically elevated levels of GADD34 in *Mist1*$^{-/-}$ mice may be responsible for the adaptation of the PERK arm of the UPR. Ongoing studies in our lab are examining the molecular links between *Gadd34* and *Mist1* for a better understanding of the relationship between MIST1 and mediators of the UPR. Treatment with the pharmacological agent, salubrinal, which selectively inhibits the dephosphorylation of eIF2α by the GADD34/PP1 complex (Boyce et al, 2005) followed by analysis of

parameters of pancreatic injury will provide clues as to the importance of GADD34 in the *Mist1*$^{-/-}$ phenotype.

Seemingly, the lack of MIST1, either directly or through secondary effects, is the trigger for activating the UPR in *Mist1*$^{-/-}$ mice, but the inability of the UPR to immediately ameliorate this stress eventually leads to its attenuation, which in turn can be beneficial to the cell by releasing translational attenuation. Whether suppression of the UPR is directly protective against pancreatic injury in *Mist1*$^{-/-}$ mice is currently unclear. It is very likely that other mechanisms (such as the inflammatory pathway involving NF-κB) also play a role in preventing the pancreatitis-like phenotype in these mice. Further work is warranted to determine the molecular events involved in the attenuation of UPR activity between 2 and 6 months of age in the *Mist1*$^{-/-}$ pancreas as well as uncover other pathways that may be activated to protect the tissue.

4.2.3 Diets high in ethanol and fat activate the UPR in pancreatic acinar cells

Consistent with recent evidence of UPR activation in the pancreas triggered by ethanol feeding (Lugea et al, 2011), the findings in this thesis show that an ethanol diet enhances activity of the IRE1 and PERK arms of the UPR. Furthermore, a high-fat diet also causes increased activation of the UPR, signifying a novel finding. Additionally, ethanol and high-fat feeding caused no discernible damage to pancreatic morphology in

WT tissue. This also agrees with the finding that activation of the UPR protects the pancreas from ethanol induced damage (Lugea et al, 2011). One difference however, is that the Lugea et al (2011) study detected a significant increase only in *sXbp1* in response to ethanol feeding of wild type mice while this project has identified a significant increase in peIF2α as well. The fact that Lugea et al (2011) employed the French-Tsukamoto model of continuous intragastric ethanol fusion, resulting in increased exposure to ethanol may account for the observed discrepancies.

As a potential output of the UPR, acinar autophagy was examined in response to high-fat and ethanol feeding. Autophagy is an essential cellular degradation mechanism. By triggering cell autophagy, non-essential organelles are processed to re-use micromolecular nutrients under conditions of stress (Levine & Klionsky, 2004). Recent studies have shown that ER stress can trigger autophagy in an *Atg* (autophagy related gene)-related manner through the UPR (Yorimitsu et al, 2006). UPR induced autophagy is mediated by PERK and the IRE1 pathways and plays a cytoprotective role in the face of severe ER stress (Ogata et al, 2006; Yorimitsu et al, 2006). In addition, Lugea et al (2011) observed a modest increase in autophagy in ethanol fed pancreatic tissue and a lack of overt morphological damage due to ethanol treatment. Given these studies, I hypothesized that chronic ethanol and high fat feeding should induce acinar autophagy by induction of ER stress and activation of the UPR. The findings in this project indicate that the high-fat diet causes a significant increase in autophagy in wild type pancreatic tissue, while ethanol causes a modest increase. This is consistent with

activation of both the PERK and IRE1 arms of the UPR in response to diet and correlates with a lack of inflammation in WT mice on either diet.

4.2.4 Long term exposure to ethanol leads to attenuation of the UPR in *Mist1*$^{-/-}$ pancreatic acinar cells.

The findings in this thesis indicate that chronic ethanol exposure resulted in decreased activation of the UPR in *Mist1*$^{-/-}$ mice. A significant decrease in *sXbp1* mRNA levels was observed in response to ethanol alone. Interestingly, both LDC-C and LDC-E diets appeared to reduce overall *Xbp1* accumulation, which is a target of ATF6α trans-activation (Wang et al, 2000). Additionally, both diets caused a significant decrease in levels of the ER chaperone, BiP/GRP78 which is also a target of ATF6 signaling (Wang et al, 2000) while peIF2α levels were unchanged in response to either diet. Taken together, these results suggest that *Mist1*$^{-/-}$ mice had a reduction in ATF6 signaling as a result of ethanol or high-fat consumption, while IRE1 signaling is perturbed only in response to ethanol. A closer look at the relationship between MIST1 and UPR signaling may provide more insight into this effect.

Mist1$^{-/-}$ mice exhibit an altered UPR in response to induction of acute pancreatitis (Kowalik et al, 2007) and recent studies have shown that activation of the UPR is a

protective response to chronic alcohol exposure (Lugea et al, 2011). Therefore, the inability to activate this pathway in *Mist1*$^{-/-}$ mice in response to environmental stressors would be detrimental to the pancreas. Examination of *Mist1*$^{-/-}$ pancreas revealed that *Xbp1* splicing in *Mist1*$^{-/-}$ mice is significantly reduced compared to that in both LDC-C and breeder chow fed *Mist1*$^{-/-}$ mice, while the LDC diets alone (both HF and E) led to increased *Xbp1* splicing relative to breeder chow fed WT mice. Examination of the PERK pathway revealed a trend where the LDC-E and LDC-C fed *Mist1*$^{-/-}$ mice contained similar levels of peIF2α protein compared to LDC-C and breeder chow fed *Mist1*$^{-/-}$ mice, indicating an inability to activate this pathway. This suggests that chronic activation of the pathway may cause an adaptive effect that alters the response of the cells to additional stress events. However, the fact that inflammation was observed only in the LDC-E fed mice suggests that it is the specific loss of *sXbp1* mRNA that is responsible for this outcome.

Recent studies have shown that XBP1 can directly bind a *cis*-regulatory sequence in the *Mist1* promoter (in the stomach) and is required for the induction of MIST1 in vivo (Huh et al, 2010). Interestingly, MIST1 expression is maintained in gastric zymogenic cells even upon loss of XBP1 (Huh et al, 2010). The idea that *Mist1* is a direct transcriptional target of *Xbp1* provides novel links between a key UPR mediator and a transcription factor required for normal pancreatic function. Lack of XBP1 in the pancreas (as in *XBP1*$^{-/-}$*;Liv*^{XBP1} mouse with liver-specific rescue of XBP1 expression) resulted in severe deficits in the exocrine pancreas including pronounced decreases in

the production of digestive enzymes, an under-developed endoplasmic reticulum and massive apoptosis during development (Lee et al, 2005). More recently, pancreatic acinar cell specific ablation of XBP1 has been demonstrated to be lethal to acinar cells, resulting in ER stress, loss of zymogen granules (and MIST1 expression) and acinar ultra-structure, reduction in the enzymes, amylase and elastase and premature activation of the digestive enzyme, carboxypeptidase (CPA) (Hess et al, 2011). Hence, in addition to its role in the cellular response to ER stress, XBP1 is also important for normal pancreatic acinar cell development and function. These findings in concert suggest that the loss of *sXbp1* observed in LDC-E fed *Mist1*$^{-/-}$ mice is a likely cause of pancreatic damage observed in these mice. Given that the Mist1 gene is a target for XBP1 transcriptional regulation (Huh et al, 2010), the simplest model would suggest that MIST1 mediates part of XBP1's protective effect against ethanol feeding. However, there are strong arguments against this theory. First, *Xbp1* splicing is enhanced in *Mist1*$^{-/-}$ tissue under non-experimental conditions and decreases after exposure to ethanol. Secondly, MIST1 is normally expressed to high levels in pancreatic tissue, even in the absence of *Xbp1* splicing. Third, work in our lab has recently uncovered an inhibitory role for XBP1 on *Mist1* gene activity, suggesting that MIST1 does not mediate the effects of XBP1 under conditions of stress in pancreatic acinar cells (Fazio E, personal communication).

An alternative scenario is that *Mist1*$^{-/-}$ acinar cells adapt to chronic stress by repressing the various UPR pathways. Although *Mist1*$^{-/-}$ mice show inhibition of the UPR in response to acute CIP (Kowalik et al, 2007) and age-dependent attenuation over

time, it is likely that mediators of the ER stress response are not targets of MIST1 transcriptional regulation. Previous work on the *Mist1*$^{-/-}$ phenotype has revealed intracellular activation of digestive enzymes, cell disorganization, increased autophagy and stellate cell activation, all of which will put undue stress on the tissue. The findings indicate elevated expression or activity of each UPR pathway with GADD34 (PERK), spliced XBP1 (IRE1) and Bip/GRP78 (ATF6) in *Mist1*$^{-/-}$ tissue. However, ethanol exposure decreased the expression of BiP/GRP78 and spliced *Xbp1* over time, corresponding to appearance of inflammatory cell accumulations. It is likely that *Mist1*$^{-/-}$ acinar cells adapt to repress the deleterious consequences of chronic activation of the UPR. When a second stress, such as ethanol, is introduced, the acinar cells are unable to further activate the pathway required for protection. The elevated levels of GADD34 found in *Mist1*$^{-/-}$ tissue support such a model. Decreased accumulation of *sXbp1* and BiP/GRP78 in response to both ethanol and high fat also support a model in which the UPR cannot be properly activated. Further work is required to distinguish between the two models of relationship between MIST1 and XBP1/UPR signaling.

At this point, it is not clear if the inflammation evident in the ethanol fed *Mist1*$^{-/-}$ mice is a direct consequence of activation of UPR attenuation or alternatively, the activation of UPR mediated inflammatory pathways. There is evidence that the UPR can directly initiate inflammation through activation of the pro-inflammatory factor, NF-κB as mediated by the PERK and IRE1-JNK pathways (Zhang & Kaufman, 2008). UPR associated inflammation is especially prominent in cells with metabolic functions (Zhang & Kaufman, 2008), such as the pancreatic acinar cells. Since no additional activation of

the PERK pathway is observed in the *Mist1*$^{-/-}$ mice in response to ethanol feeding, examination of the IRE1-TRAF2-JNK pathway may help elucidate a link between the UPR and inflammation. It is also possible that changes in the cell composition of the pancreas are the source of the UPR and related inflammation.

It is interesting that the inflammation evident in the *Mist1*$^{-/-}$ pancreas is specific to the LDC-E diet. Why do the LDC-C fed *Mist1*$^{-/-}$ mice not develop inflammation? Examination of UPR induced autophagy provides some insight. The findings in this thesis show that ethanol feeding of *Mist1*$^{-/-}$ mice had little to no effect on acinar autophagy, while a high-fat diet induces significant autophagy. This discrepancy may explain the differential effects of the LDC-C and LDC-E diets on *Mist1*$^{-/-}$ pancreatic tissue and the resulting inflammation observed only in the LDC-E fed *Mist1*$^{-/-}$ mice. Studies have shown that activation of the IRE1 signaling pathway is required for ER stress induced autophagy, while PERK and ATF6 are dispensable for this pathway (Ogata et al, 2006). More importantly, autophagy induced by the UPR is crucial for cell survival during ER stress and may act as either a degradation mechanism for unfolded proteins or maintain energy homeostasis to protect against cell death (Ogata et al, 2006). Accordingly, the findings in this thesis have shown that *Mist1*$^{-/-}$ mice on the ethanol diet alone show a significant decrease in *sXbp1*, a direct target of IRE1. Considering that the increase in autophagy observed in the controls is mediated by the UPR, it seems that the LDC-E fed *Mist1*$^{-/-}$ pancreas is unable to reactivate the UPR in response to a second stressor. Given the lack of evident pancreatic injury in high fat fed

Mist1$^{-/-}$ mice, it is likely that the increase in autophagy in this case, is playing a protective role. On the other hand, lack of induction of autophagy in response to ethanol feeding in the *Mist1*$^{-/-}$ mice suggests that loss of the cytoprotective function of autophagy may be one reason for the appearance of inflammation in this group alone. Evaluation of autophagy in relation to activation of the IRE1-JNK pathway of the UPR should provide clues regarding the contribution of this process to the inflammatory pathway and the resulting phenotype.

These results suggest that the sensitivity of *Mist1*$^{-/-}$ pancreatic tissue to ethanol exposure correlates with their inability to activate the UPR. Combined, these results show that the pancreatic tissue of *Mist1*$^{-/-}$ animals has higher baseline levels of UPR, but responds to adverse conditions by reducing or suppressing further activation of the UPR. Overall, these findings highlight the role of the UPR and its outputs in mediating the course of ethanol induced pancreatic damage in the absence of a genetic factor that is crucial for pancreatic function. In addition, this work has implications for pharmacological or genetic manipulation of the UPR to ameliorate symptoms of pancreatic disease in the context of genetic mutations or deletions in human patients.

4.2.5 Chronic ethanol and high-fat exposure followed by an acute pancreatitis episode prevents further enhancement of the UPR.

The findings in this section indicate that UPR markers including BiP/GRP78, peIF2α, ATF3 and ATF4 were not significantly altered as a result of CIP in breeder chow, LDC-C or LDC-E diets, while both LDC-C and LDC-E diets led to a significant increase in pPERK activity. While this agrees with the hypothesis that the ability of LDC-C and LDC-E fed wild types to activate the UPR in the presence of additional acute stress will be compromised, it raises the question of why pPERK levels are altered while its downstream targets such as peIF2α, ATF3 and ATF4 remain unchanged. One explanation could be the time-point at which CIP was initiated. It is possible that the 4 hour duration was enough to elicit increased activity of pPERK but too early to activate its downstream targets in the UPR. Initiation of a longer duration of CIP followed by assessment of pPERK activity as well as its downstream targets may shed more light on activation of this pathway. Further work is also needed to assess activation of the IRE1 and ATF6 arms, although preliminary results suggest no differences between treatments. Given that increased activity of PERK is observed following 4 hour CIP in the WT pancreas (Kowalik et al, 2007), it is necessary to compare activation of UPR mediators between non-CIP treated (saline injected) controls with the experimental groups to provide a better understanding of the changes in UPR activity relative to starting levels. Furthermore, while preliminary histological analysis did not reveal additional damage in the LDC-E and LDC-C groups relative to the BC diet, more extensive work is required to establish a correlative link between lack of UPR

enhancement and pancreatic damage. If the LDC-E and LDC-C diet fed mice develop more pancreatic damage than the breeder chow fed counterparts, it may be interpreted as the result of lack of UPR activity due to adverse dietary conditions.

Following CIP, analysis of serum amylase levels revealed a significant decrease in response to the LDC-C diet compared to breeder chow fed controls. This finding is in contrast to a study by Ye et al (2010), where initiation of CIP in LDC-C fed WT mice caused significant increases in blood amylase and lipase levels compared to regular diet fed mice. It is likely that differences in experimental conditions, such as duration of CIP (4 hours in this project versus 7 hours), length of feeding (6 weeks in this project versus 20 weeks) and fat content in the diet (36% LDC-C versus 45%) contributed to the observed discrepancies. The findings of this project also contrast with a study by Deng et al (2005) in which LDC-E feeding of rats followed by initiation of CIP for 3 hours resulted in a significant increase in serum amylase levels in both LDC-C and LDC-E diets relative to saline-treated controls, but not relative to each other. While the dosage of cerulein (20 µg/kg body weight versus 50 µg/kg in this project) and the different animal model used (rats versus mice) could account for the observed discrepancies, it is more likely that repeated experiments with a larger n value will yield more reliable results.

Taken together, the findings in this thesis project suggest that lack of MIST1 is a risk factor for developing ethanol induced inflammation in the pancreas. Although 75%

of cases of acute pancreatitis are associated with alcohol abuse, only a small percent of heavy alcohol abusers go on to develop pancreatitis (Saluja & Bhagat, 2003). This work provides a novel genetic link that accounts for the variable response of individuals to ethanol abuse. These results can be applied to a clinical situation where human patients with deletions or mutations in *Mist1* will be placed at increased risk for developing alcohol induced pancreatitis. Referring to the current model of alcohol induced pancreatitis (Figure 1.2), this work has identified *Mist1* as one genetic trigger or co-factor that sensitizes the acinar cell to further insult in the presence of ethanol. Ongoing studies in our lab are examining pancreatic samples from patients with chronic pancreatitis for expression of MIST1. There is preliminary evidence to suggest that these patients have decreased expression of the MIST1 protein, indicating a correlative relationship with the disease phenotype at the very least. Further information on the etiology of the disease and genetic analysis of DNA from these patients should help elucidate a link between alcohol abuse, MIST1 and the risk of developing chronic pancreatitis.

In conclusion, altered MIST1 function may be an underlying cause for pancreatitis susceptibility from environmental stressors such as a diet high in fat and/or ethanol. This work provides clues as to why some individuals are more susceptible than others in developing alcoholic pancreatitis. Work in this field should also shed more light on how disease phenotypes are affected by gene-environment influences and enhance our understanding of the molecular mechanisms of pancreatic disease.

5.0 References

Acosta-Alvear D, Zhou Y, Blais A, Tsikitis M, Lents NH, Arias C, Lennon CJ, Kluger Y, Dynlacht BD. XBP1 Controls Diverse Cell Type- and Condition-Specific Transcriptional Regulatory Networks. *Molecular Cell.* 27: 53–66, 2007.

Adams GA, Rose JK. Incorporation of a charged amino acid into the membrane-spanning domain blocks cell surface transport but not membrane anchoring of a viral glycoprotein, *Mol. Cell Biol.* 5: 1442–1448, 1985.

Ammann RW. The natural history of alcoholic chronic pancreatitis. *Intern Med.* 368–375, 2001.

Andrzejewska A, Dlugosz JW, Jurkowska G. The effect of antecedent acute ethanol ingestion on the pancreas ultrastructure in taurocholate pancreatitis in rats. *Exp Mol Pathol.* 65:64-77, 1998.

Apte MV, Wilson JS, McCaughan GW et al. Ethanol-induced alterations in messenger RNA levels correlate with glandular content of pancreatic enzymes. *J. Lab. Clin. Med.* 125: 634–40, 1995.

Apte M, Haber P, Applegate T et al. Generation of fatty acid ethyl esters by rat pancreatic acini: comparison of oxidative and non-oxidative ethanol metabolism. *Gastroenterology.* 112:A426, 1997.

Barnes PJ, Karin M. Nuclear factor kappaB--a pivotal transcription factor in chronic inflammatory disease. *N Engl J Med.* 336:1066-1071, 1997.

Bhatia M. Apoptosis versus necrosis in acute pancreatitis. *Am J Physiol Gastrointest Liver Physiol* 286: G189–G196, 2004.

Boyce M, Bryant KF, Jousse C, Long K, Harding HP, Scheuner D, Kaufman RJ, Ma D, Coen, DM, Ron D et al. A selective inhibitor of eIF2alpha dephosphorylation protects cells from ER stress. *Science.* 307: 935-939, 2005.

Calfon M, Zeng H, Urano F, Till JH, Hubbard SR, Harding HP, Clark SG, Ron D. IRE1 couples endoplasmic reticulum load to secretory capacity by processing the XBP-1 mRNA. *Nature.* 415:92–96, 2002.

Case M. Synthesis, intracellular transport and discharge of exportable proteins in the pancreatic acinar cell and other cells. *Biol. Rev.* 53:211-254, 1978.

Connor JH, Weiser DC, Li S, Hallenbeck JM, Shenolikar S. Growth arrest and DNA damage-inducible protein GADD34 assembles a novel signaling complex containing protein phosphatase 1 and inhibitor 1. *Mol Cell Biol.* 21(20):6841-50, 2001.

Cosen-Binker LI, Lam PPL, Binker MG, Gaisano HY. Alcohol-Induced Protein Kinase C_ Phosphorylation of Munc18c in Carbachol-Stimulated Acini Causes Basolateral Exocytosis. *Gastroenterology*. 132:1527–1545, 2007.

Cox JS, Shamu CE, Walter P. Transcriptional induction of genes encoding endoplasmic reticulum resident proteins requires a transmembrane protein kinase. *Cell*. 73:1197–1206, 1993.

Criddle DN, Murphy J, Fistetto G et al. Fatty acid ethyl esters cause pancreatic calcium toxicity via inositol trisphosphate receptors and loss of ATP synthesis. *Gastroenterology*.130: 781–93, 2006.

Deng X, Wang L, Elm MS, Gabazadeh D, Diorio GJ, Eagon PK, Whitcomb DC. Chronic Alcohol Consumption Accelerates Fibrosis in Response to Cerulein-Induced Pancreatitis in Rats. *Am J Pathol*. 166(1): 93–106, 2005.

Elayat AA, el-Naggar MM, Tahir M. An immunocytochemical and morphometric study of the rat pancreatic islets. *Journal of Anatomy*. 186 (Pt 3): 629–37, 1995.

Fernández-Sánchez M, del Castillo-Vaquero A, Salido GM, González A. Ethanol exerts dual effects on calcium homeostasis in CCK-8-stimulated mouse pancreatic acinar cells. *BMC CellBiol*. 10: 77, 2009.

Figarella C, Miszczuk-Jamska B, Barrett AJ. Possible lysosomal activation of pancreatic zymogens. Activation of both human trypsinogens by cathepsin B and spontaneous acid. Activation of human trypsinogen 1. *Biol Chem Hoppe Seyler*. 369: 293–298, 1988.

Glasbrenner B, Adler G. Pathophysiology of acute pancreatitis. *Hepatogastroenterology*. 40: 517-521, 1993.

González A, Núñez AM, Granados MP, Pariente JA, Salido GM. Ethanol impairs CCK-8-evoked amylase secretion through Ca2+-mediated ROS generation in mouse pancreatic acinar cells. *Alcohol*. 38: 51-57, 2006.

Gorry MC, Gabbaizedeh D, Furey W et al. Mutations in the cationic trypsinogen gene are associated with recurrent acute and chronic pancreatitis. *Gastroenterology* 113(4):1063–68, 1997.

Gething MJ, McCammon K, Sambrook J. Expression of wild-type and mutant forms of influenza hemagglutinin: the role of folding in intracellular transport. *Cell*. 46:939–950, 1986.

Gorelick FS, Thrower E. The Acinar Cell and Early Pancreatitis Responses. *Clinical Gastroenterology and Hepatology*. 7:S10–S14, 2009.

Greenbaum LM, Hirshkowitz A, Shoichet I. The activation of trypsinogen by cathepsin B. *J Biol Chem* 234: 2885–2890, 1959.

Gukovskaya AS, Mouria M, Gukovsky I et al. Ethanol metabolism and transcription factor activation in pancreatic acinar cells in rats. *Gastroenterology.* 122: 106–18, 2002.

Haber PS, Wilson JS, Apte MV, et al. Fatty acid ethyl esters increase rat pancreatic lysosomal fragility. *J Lab Clin Med.* 121:759–764, 1993.

Haber PS, Apte MV, Applegate TL et al. Metabolism of ethanol by rat pancreatic acinar cells. *J. Lab. Clin. Med.* 132: 294–302, 1998.

Hand AR. The secretory process of salivary glands and pancreas. In: *Ultrastructure of the Extraparietal Glands of the Digestive Tract.* A. Riva and P.M. Motta, eds. Kluwer, Boston, pp. 1–17, 1990.

Harding HP, Zhang Y, Ron D. Protein translation and folding are coupled by an endoplasmic reticulum- resident kinase. *Nature.* 397:271–274, 1999.

Harding HP, Zhang Y, Bertolotti A, Zeng H, Ron D. *Perk* is essential for translational regulation and cell survival during the unfolded protein response. *Mol. Cell.* 5:897–904, 2000.

Harding HP, Novoa I, Zhang Y, Zeng H, Wek R, Schapira M, Ron D. Regulated translation initiation controls stress-induced gene expression in mammalian cells. *Mol. Cell.* 6:1099–1108, 2000.

Harding HP, Zeng H, Zhang Y, Jungries R, Chung P, Plesken H, Sabatini DD, Ron D. Diabetes mellitus and exocrine pancreatic dysfunction in perk-/- mice reveals a role for translational control in secretory cell survival. *Mol. Cell.* 7(6):1153-1163, 2001.

Haze K, Yoshida H, Yanagi H, Yura T, Mori K. Mammalian transcription factor ATF6 is synthesized as a transmembrane protein and activated by proteolysis in response to endoplasmic reticulum stress. *Mol. Biol. Cell.* 10: 3787–3799, 1999.

Haze K, Okada T, Yoshida H, Yanagi H, Yura T, Negishi M, Mori K. Identification of the G13 (cAMP-response-elementbinding protein-related protein) gene product related to activating transcription factor 6 as a transcriptional activator of the mammalian unfolded protein response, *Biochem. J.* 355:19–28, 2001.

Hess DA, Humphrey SE, Ishibashi J, Damsz B, Lee AH, Glimcher LH, Konieczny SF. Extensive Pancreas Regeneration Following Acinar-Specific Disruption of Xbp1 in Mice. *Gastroenterology.* Accepted Manuscript, 2011.

Hinnebusch AG. Translational regulation of yeast GCN4. A window on factors that control initiator-tRNA binding to the ribosome. *J. Biol. Chem.* 27:21661–21664, 1997.

Huh WJ, Esen E, Geahlen JH, Bredemeyer AJ, Lee AH, Shi G, Konieczny SF, Glimcher LH, Mills JC. XBP1 Controls Maturation of Gastric Zymogenic Cells by Induction of MIST1 and Expansion of the Rough Endoplasmic Reticulum. *Gastroenterology*. 139(6):2038-2049, 2010.

Iumuro Y, Bradford BU, Yamashina S, Rusyn I, Nakagami M, Enomoto N, Kon H, Frey W, Forman D, Brenner D, Thurman RG. The glutathione precursor 1,2-oxothiazolidine-4- carboxylic acid protects against liver injury due to chronic ethanol exposure in the rat. *Hepatology*. 31: 391-398, 2000.

Jiang HY, Wek SA, McGrath BC, Lu D, Hai T, Harding HP, Wang X, Ron D, Cavener DR, Wek RC. Activating transcription factor 3 is integral to the eukaryotic initiation factor 2 kinase stress response. *Mol. Cell Biol.* 24:1365–1377, 2004.

Johnson CL, Kowalik AS, Rajakumar N, Pin CL. Mist1 is necessary for the establishment of granule organization in serous exocrine cells of the gastrointestinal tract. *Mechanisms of development*. 121, 261-272, 2004.

Juarez J, Barrios de Tomasi E. Sex differences in alcohol drinking patterns during forced and voluntary consumption in rats. *Alcohol*. 19:15-22, 1999.

Kaser, A., Lee, A. H., Franke, A., Glickman, J. N., Zeissig, S., Tilg, H., Nieuwenhuis, E. E., Higgins, D. E., Schreiber, S., Glimcher, L. H., and Blumberg, R. S. XBP1 links ER stress to intesti-nal inflammation and confers genetic risk for human inflammatory bowel disease. *Cell*. 134:743–756, 2008.

Keane B, Leonard BE. Rodent models of alcoholism: a review. *Alcohol and Alcoholism*. 24: 299-309)

Kempen HJM, de Pont, JJHHM, Bontin SL. Rat pancreas adenylate cyclase. V. Its presence in isolated rat pancreatic acinar cells. *Biochim Biophys Acta*. 486: 521-31, 1977.

Kimura T, Imamura K, Eckhardt L, Schulz I. Ca2+-, phorbol ester-, and cAMP-stimulated enzyme secretion from permeabilized rat pancreatic acini. *Am J Physiol*. 250, G698-708, 1986.

Kowalik AS, Johnson CL, Chadi SA, Weston J, Fazio EN, Pin CL. Mice lacking the transcription factor Mist1 exhibit an altered stress response and increased sensitivity to caerulein-induced pancreatitis. *Am J Physiol Gastrointest Liver Physiol.* 292:1123-1132, 2007.

Kozutsumi Y, Segal M, Normington, Gething MJ, Sambrook J. The presence of malfolded proteins in the endoplasmic reticulum signals the induction of glucose-regulated proteins. *Nature*. 332: 462–464, 1988.

Kruger B, Albrecht E, Lerch MM. The role of intracellular calcium signaling in premature protease activation and the onset of pancreatitis. *Am J Pathol.* 157:43-50, 2000.

Kubisch CH, Sans MD, Arumugam T, Ernst SA, Williams JA, Logsdon CD. Early activation of endoplasmic reticulum stress is associated with arginine-induced acute pancreatitis. *Am J Physiol Gastrointest Liver Physiol.* 291 (2): G238-G245, 2006.

Kuijpers GAJ, de Pont JJHHM. Role of proton and bicarbonate transport in pancreatic cell function. *Annu Rev Physiol.* 49: 87-103, 1987.

Lee AH, Chu GC, Iwakoshi NN, Glimcher LH. XBP-1 is required for biogenesis of cellular secretory machinery of exocrine glands. *The EMBO Journal.* 24: 4368–4380, 2005.

Lemercier C, To RQ, Swanson BJ, Lyons GE, Konieczny SF. Mist1: a novel basic helix–loop–helix transcription factor exhibits a developmentally regulated expression pattern. *Dev. Biol.* 182: 101–113, 1997

Levine B, Klionsky DJ. Development by self-digestion: molecular mechanisms and biological functions of autophagy. *Dev. Cell.* 6:463–477, 2004.

Lieber CS, DeCarli LM. The feeding of alcohol in liquid diets. *Alcohol Clin Exp Res.* 10:550–553, 1986.

Lodish H, Berk A, Zipursky SL, et al. *Molecular Cell Biology.* 4th edition. New York: W. H. Freeman, 2000.

Logsdon CD. Molecular structure and function of G-protein-linked receptors. Johnson LR, ed. *Physiology of the Gastrointestinal Tract*, Vol. 2. New York: Raven. 3rd. ed. 2202 pp. 351–80, 1994.

Logsdon CD. Signal transduction in pancreatic acinar cell physiology and pathophysiology. *Current Opinion in Gastroenterology.* 16:404–409, 2000.

Luo X, Shin DM, Wang X, Konieczny SF, Muallem S. Aberrant Localization of Intracellular Organelles, Ca^{2+}Signaling, and Exocytosis in Mist1 Null Mice. *The Journal of Biological Chemistry.* 280 (13): 12668–12675, 2005.

Lugea A, Tischler D, Nguyen J, Gong J, Gukovsky I, French SW, Gorelick FS, Pandol SJ. Adaptive unfolded protein response attenuates alcohol-induced pancreatic damage. *Gastroenterology.* 140(3):987-97, 2011.

Maeda K, Hirota M, Kimura Y, Ichihara A, Ohmuraya M, Sugita H et al. Pro-inflammatory role of trypsin and protease activated receptor-2 in rat model of acute pancreatitis. *Pancreas.* 31:54–62, 2005.

Maisonneuve P, Lowenfels AB, Mullhaupt B et al. Cigarette smoking accelerates progression of alcoholic chronic pancreatitis. *Gut.* 54:510–514, 2005.

Matozaki T, Goke B, Tsunoda Y, Rodriguez M, Martinez J, Williams, JA. Two functionally distinct cholecystokinin receptors show different modes of action on Ca2+ mobilization and phospholipid hydrolysis in isolated rat pancreatic acini. Studies using a new cholecystokinin analog, JMV-180. *J Biol Chem.* 265: 6247-54, 1990.

Mori K, Ma W, Gething MJ, Sambrook J. A transmembrane protein with a cdc2+/CDC28-related kinase activity is required for signaling from the ER to the nucleus. *Cell.* 74**:** 743–756, 1993.

Mori K, Ogawa N, Kawahara T, Yanagi H, Yura T. Palindrome with spacer of one nucleotide is characteristic of the *cis*-acting unfolded protein response element in *Saccharomyces cerevisiae*. *J. Biol. Chem.* 273:9912–9920, 1998.

Murphy JA, Criddle DN, Sherwood M, et al. Direct activation of cytosolic Ca2+ signaling and enzyme secretion by cholecystokinin in human pancreatic acinar cells. *Gastroenterology.* 135:632–641, 2008.

Nordback IH, MacGowan S, Potter J *et al.* The role of acetaldehyde in the pathogenesis of acute alcoholic pancreatitis. *Ann. Surg.* 214: 671–8, 1991.

Norton ID, Apte MV, Lux O, et al. Chronic ethanol administration causes oxidative stress in the rat pancreas. *J Lab Clin Med.* 131:442–446, 1998.

Ogata M, Hino S, Saito A, Morikawa K, Kondo S, Kanemoto S et al. Autophagy is activated for cell survival after endoplasmic reticulum stress. *Mol Cell Biol.* 26: 9220–9231, 2006.

Ohmuraya M, Hirota M, Araki M, Mizushima N, Matsui M, Mizumoto T et al. Autophagic cell death of pancreatic acinar cells in serine protease inhibitor Kazal type 3-deficient mice. *Gastroenterology.* 129:696–705, 2005.

Owyang C. Physiological mechanisms of cholecystokinin action on pancreatic secretion. *Am J Physiol.* 1(1):G1–G7, 1996.

Oyadomari S, Mori M. Roles of CHOP/ GADD153 in endoplasmic reticulum stress. *Cell Death Differ.* 11:381–389, 2004.

Pandol SJ, Periskic S, Gukovsky I, Zaninovic V, Jung Y, Zong Y, Solomon TE, Gukovskaya AS, Tsukamoto H. Ethanol diet increases the sensitivity of rats to pancreatitis induced by cholecystokinin octapeptide. *Gastroenterology*. 117(3):706-16, 1999.

Pandol SJ, Gukovsky I, Satoh A, Lugea A, Gukovskaya AS. Animal and in vitro models of alcoholic pancreatitis: role of cholecystokinin. *Pancreas.* 27:297-300, 2003

Pandol SJ, Gorelick FS, Lugea A. Environmental and genetic stressors and the unfolded protein response in exocrine pancreatic function – a hypothesis. *Frontiers in Physiology*. 2 (8): 1-7, 2011.

Papa FR, Zhang C, Shokat K, Walter P. Bypassing a kinase activity with an ATP-competitive drug. *Science.* 302:1533–1537, 2003.

Perides G, Tao X, West N, Sharma A, Steer ML. A mouse model of ethanol dependent pancreatic fibrosis. *Gut*. 54:1461–1467, 2005.

Pin CL, Bonvissuto AC, Konieczny SF. Mist1 expression is a common link among serous exocrine cells exhibiting regulated exocytosis. *Anat Rec.* 259: 157–167, 2000.

Pin CL, Rukstalis JM, Johnson C, Konieczny SF. The bHLH transcription factor Mist1 is required to maintain exocrine pancreas cell organization and acinar cell identity. *J Cell Biol.* 155: 519–530, 2001.

Ponnappa BC, Hoek JB, Waring AJ et al. Effect of ethanol on amylase secretion and cellular calcium homeostasis in pancreatic acini from normal and ethanol-fed rats. *Biochem. Pharmacol.* 36: 69–79, 1987.

Raraty M, Ward J, Erdemli G et al. Calcium-dependent enzyme activation and vacuole formation in the apical granular region of pancreatic acinar cells. *Proc Natl Acad Sci USA*. 97:13126-31, 2000.

Reimold AM, Etkin A, Clauss I, Perkins A, Friend DS, Zhang J, Horton HF, Scott A, Orkin SH, Byrne MC et al. An essential role in liver development for transcription factor XBP-1. *Genes Dev.* **14:** 152–157, 2000.

Rinderknechht H, Engelinge R, Bunnell MJ, Geokas MC. A sensitive assay for human enterokinase and some properties of the enzyme. *Clinica Chimica Acta.* 3: 145-160, 1974.

Rosendahl J, Witt H, Szmola R et al. Chymotrypsin C (CTRC) variants that diminish activity or secretion are associated with chronic pancreatitis. *Nat. Genet.* 40(1):78–82, 2008.

Rukstalis JM, Kowalik A, Zhu L, Lidington D, Pin CL., Konieczny SF. Exocrine specific expression of connexin32 is dependent on the basic helix-loop- helix transcription factor Mist1. *J Cell Sci.* 116: 3315–3325, 2003.

Saluja A, Saito I, Saluja M, Houlihan MJ, Powers RE, Meldolesi J, Steer M. In vivo rat pancreatic acinar cell function during supramaximal stimulation with caerulein. *Am J Physiol Gastrointest Liver Physiol.* 249: G702–G710, 1985.

Saluja A, Hashimoto S, Saluja M, Powers RE, Meldolesi J, Steer ML. Subcellular redistribution of lysosomal enzymes during caerulein-induced pancreatitis. *Am J Physiol Gastrointest Liver Physiol.* 253: G508–G516, 1987.

Sankaran H, Lewin MB, Wong A et al. Irreversible inhibition by acetaldehyde of cholecystokinin-induced amylase secretion from isolated rat pancreatic acini. *Biochem. Pharmacol.* 34: 2859–63, 1985.

Sans MD, Dimagno MJ, D'Alecy LG, and Williams JA. Caerulein-induced acute pancreatitis inhibits protein synthesis through effects on eIF2B and eIF4F. *Am J Physiol Gastrointest Liver Physiol.* 285: G517–G528, 2003.

Sarles H, Sarles JC, Cammate R, Muratore R, Gaini M, Guein C, Pastor J, Le Roy F. Observation of 205 confirmed cases of acute pancreatitis, recurring pancreatitis, and chronic pancreatitis. *Gut.* 6:545-559, 1965.

Scheele G, Adler G, Kern H. Exocytosis occurs at the lateral plasma membrane of the pancreatic acinar cell during supramaximal secretagogue stimulation. *Gastroenterology.* 92:345-53, 1987.

Scheuner D, Song B, McEwen E, Liu C, Laybutt R, Gillespie P, Saunders T, Bonner-Weir S, Kaufman RJ. Translational control is required for the unfolded protein response and in vivo glucose homeostasis. *Mol. Cell.* 7:1165–1176, 2001.

Schneider A, Whitcomb DC, Singer MV. Animal models in alcoholic pancreatitis _ what can we learn? *Pancreatology.* 2:189-203, 2002.

Schröder M, Chang JS, Kaufman RJ, The unfolded protein response represses nitrogen-starvation induced developmental differentiation in yeast. *Genes Dev.* 14: 2962–2975, 2000.

Schröder M, Kaufman RJ. Divergent roles of Ire1 and PERK in the unfolded protein response. *Curr. Mol. Med.* 6:5–36, 2006.

Sharma A, Tao X, Gopal A, Ligon B, Andrade-Gordon P, Steer ML et al. Protection against acute pancreatitis by activation of protease-activated receptor-2. *Am J Physiol.* 288:G388– 95, 2005.

Shi Y, Vattem KM, Sood R, An J, Liang J, Stramm L, Wek RC. Identification and characterization of pancreatic eukaryotic initiation factor 2-subunit kinase, PEK, involved in translational control. *Mol. Cell Biol.* 18: 7499–7509, 1998.

Shi Y, An J, Liang J, Hayes SE, Sandusky GE, Stramm LE, Yang NN. Characterization of a mutant pancreatic eIF-2kinase, PEK, and co-localization with somatostatin in islet delta cells. *J. Biol. Chem.* 274:5723–5730, 1999.

Siech M, Heinrich P, Letko G. Development of acutecpancreatitis in rats after single ethanol administration andcinduction of a pancreatic juice edema. *Int J Pancreatol.* 8:169-75, 1991.

Simon P, Weiss FU, Zimmer KP, et al. Acute and chronic pancreatitis in patients with inborn errors of metabolism. *Pancreatology.* 1(5):448–56, 2001.

Slack JM. Developmental biology of the pancreas. *Development.* 121: 1569-80, 1995.

Steer ML, Meldolesi J. The cell biology of experimental pancreatitis. *N Engl J Med.* 316:144-50, 1988.

Steer ML, Meldolesi J. Pathogenesis of acute pancreatitis. *Annual Rev Med.* 39: 95-105, 1988.

Sampson HW, Chaffin C, Lange J, DeeFee B. Alcohol consumption by young actively growing rats: A histomorphometric study of cancellous bone. *Alcoholism: Clinical and Experimental Research*. 21:352-358, 1997.

Sidrauski C, Cox JS, Walter P. tRNA ligase is required for regulated mRNA splicing in the unfolded protein response. *Cell.* 87:405–413, 1996.

Su KH, Cuthbertson C, Christophi C. Review of experimental animal models of acute pancreatitis. *HPB.* 8: 264-286, 2006.

Sudhof T. The synaptic vesicle cycle: a cascade of protein-protein interactions. *Nature* 375:645–63, 1995.

Thorn P, Lawrie AM, Smith PM, Gallacher DV, Petersen OH. Ca^{2+} oscillations in pancreatic acinar cells: spatiotemporal relationships and functional implications. *Cell Calcium.* 14(10):746-57, 1993.

Tian X, Jin RU, Bredemeyer AJ, Oates EJ, Błażewska KM, McKenna CE, Mills JC. RAB26 and RAB3D are direct transcriptional targets of MIST1 that regulate exocrine granule maturation. *Mol Cell Biol.* 30(5): 1269–1284, 2010.

Tirasophon, W, Lee K., Callaghan B, Welihinda A, Kaufman RJ. The endoribonuclease activity of mammalian IRE1 autoregulates its mRNA and is required for the unfolded protein response. *Genes Dev.* 14:2725–2736, 2000.

Urano F, Wang X, Bertolotti A, Zhang Y, Chung P, Harding HP, Ron D. Coupling of stress in the ER to activation of JNK protein kinases by transmembrane protein kinase IRE1, *Science.* **287**: 664–666, 2000.

Vonlaufen A, Wilson JS, Pirola RC, Apte MV. Role of alcohol metabolism in chronic pancreatitis. *Alcohol Res Health*. 30(1):48-54, 2007.

Van Acker GJD, Weiss E, Steer ML, Perides G. Cause-effect relationships between zymogen activation and other early events in secretagogue-induced acute pancreatitis. *Am J Physiol Gastrointest Liver Physiol.* 292: G1738–G1746, 2007.

Wang XZ, Harding HP, Zhang Y, Jolicoeur EM, Kuroda M, Ron D. Cloning of mammalian Ire1 reveals diversity in the ER stress responses, *EMBO J.* 17:5708–5717, 1998.

Wang Y, Sternfeld L, Yang F et al. Enhanced susceptibility to pancreatitis in severe hypertriglyceridaemic lipoprotein lipase-deficient mice and agonist-like function of pancreatic lipase in pancreatic cells. *Gut.* 58(3):422–30, 2009.

Wang Y, Shen J, Arenzana N, Tirasophon, W, Kaufman RJ, Prywes, R. Activation of ATF6 and an ATF6 DNA binding site by the endoplasmic reticulum stress response. *J. Biol. Chem.* 275(27):013–27, 2000.

Wasle B, Edwardson JM. The regulation of exocytosis in the pancreatic acinar cell. *Cell Signal.* 14: 191-197, 2002.

Watanabe O, Baccino FM, Steer ML, Meldolesi J. Supramaximal caerulein stimulation and ultrastructure of rat pancreatic acinar cell: early morphological changes during development of experimental pancreatitis. *Am J Physiol Gastrointest Liver Physiol* 246: G457–G467, 1984

Werner J, Laposata M, Fernandez-del Castillo C et al. Pancreatic injury in rats induced by fatty acid ethyl ester, a nonoxidative metabolite of alcohol. *Gastroenterology.* 113:286–294, 1997.

Werner J, Saghir M, Warshaw AL et al. Alcoholic pancreatitis in rats: Injury from nonoxidative metabolites of ethanol. *Am J Physiol Gastrointest Liver Physiol.* 283:G65–G73, 2002.

Whitcomb DC, Gorry MC, Preston RA et al. Hereditary pancreatitis is caused by a mutation on the cationic trypsinogen gene. *Nat Genet.* 14:141–145, 1996.

Willemer S, Bialek R, Adler G. Localization of lysosomal and digestive enzymes in cytoplasmic vacuoles in caerulein-pancreatitis. *Histochemistry*. 94:161-70, 1990.

Wilson DE, Hata A, Kwong LK, et al. Mutations in exon 3 of the lipoprotein lipase gene segregating in a family with hypertriglyceridemia, pancreatitis, and non-insulin-dependent diabetes. *J. Clin. Invest.* 92(1):203–11, 1993.

Witt H, Luck W, Hennies HC, Classen M, Kage A, Lass U, et al. Mutations in the gene encoding the serine protease inhibitor, Kazal type 1 are associated with chronic pancreatitis. *Nat Genet.* 25:213–6, 2000.

Wu D, Rutkowski T, Dubois M, Swathirajan J, Saunders T, Wang J, Song B, Yau GDY, Kaufman RJ. ATF6alpha optimizes long-term endoplasmic reticulum function to protect cells from chronic stress. *Dev. Cell.* **13**: 351–364, 2007.

Yamamoto K, Sato T, Matsui T, Sato M, Okada T, Yoshida H, Harada A, Mori K. *Dev. Cell.* **13**: 365–376, 2007.

Ye R, Mareninova OA, Barron E, Wang , Hinton DR, Pandol SJ, Lee AS. *Grp78* Heterozygosity Regulates Chaperone Balance in Exocrine Pancreas with Differential Response to Cerulein-Induced Acute Pancreatitis. *The American Journal of Pathology.* 177 (6): 2827-2836, 2010.

Ye J, Rawson RB, Komuro R, et al. ER stress induces cleavage of membrane-bound ATF6 by the same proteases that process SREBPs. *Mol. Cell.* 6:1355–1364, 2000.

Yorimitsu T, Nair U, Yang Z, Klionsky DJ. Endoplasmic reticulum stress triggers autophagy. *J Biol Chem.* 281: 30299–30304, 2006.

Yoshida H, Haze K, Yanagi H, Yura T, Mori K. Identification of the *cis*-acting endoplasmic reticulum stress response element responsible for transcriptional induction of mammalian glucose-regulated proteins. Involvement of basic leucine zipper transcription factors. *J. Biol. Chem.* 273, 33:741–33,749, 1998.

Yoshida H, Okada T, Haze K, et al. ATF6 activated by proteolysis binds in the presence of NFY(CBF) directly to the *cis*-acting element responsible for the mammalian unfolded protein response. *Mol. Cell. Biol.* 20:6755–6767, 2000.

Yoshida H, Matsui T, Yamamoto A, Okada T, Mori K. XBP1 mRNA is induced by ATF6 and spliced by IRE1 in response to ER stress to produce a highly active transcription factor. *Cell.* 107: 881–891, 2001.

Yule DI, Baker CW, Williams JA. Calcium signaling in rat pancreatic acinar cells: a role for Galphaq, Galpha11, and Galpha14. *Am J Physiol.* 276:G271–G279, 1999.

Zhang K & Kaufman RJ. From endoplasmic-reticulum stress to the inflammatory response. *Nature.* 454(7203): 455–462, 2008.

Zhang P, McGrath B, Li S, Frank A, Zambito F, Reinert J, Gannon M, Ma K, McNaughton K, Cavener DR. The PERK eukaryotic initiation factor 2 alpha kinase is required for the development of the skeletal system, postnatal growth, and the function and viability of the pancreas. *Mol Cell Biol.* 22(11):3864-3874, 2002.

6.0 APPENDIX

Table 2.1 Diet constituents

Composition	Research Diet #L10015		Research Diet #L10016		Teklad extruded rodent diet	
	(kcal %)		(kcal %)		(kcal %)	
Protein	17		17		23	
Carbohydrate	47		11		55	
Fat	36		36		22	
Ethanol	0		36		0	
Ingredients	gm	kcal	gm	kcal	%	
Casein	41.4	166	41.4	166	0	
DL-Methionine	0.3	1	0.3	1	0.5	
L-Cystine	0.5	2	0.5	2	0.3	
Amino acids (total)	0.8	3	0.8	3	18.5	
Maltodextrin 42	115.2	461	25.6	102	0	
Cellulose	10	0	10	0	0	
Xantham Gum	3	0	3	0	0	
Corn Oil	8.5	77	8.5	77	0	
Olive Oil	28.4	256	28.4	256	0	
Safflower Oil	2.7	24	2.7	24	0	
Fatty acids (total)					14.4	
Minerals	Salts		Salts		%	mg/kg
	8.75	0	8.75	0	3.1	361.23
Vitamins	2.5	9	2.5	9	IU/g	mg/kg
					126.5	1412.48
Choline Bitartrate	0.53	0	0.53	0	0	
Ethanol (100%)	0	0	50	360	0	

Research Diet #L10015 – Lieber-DeCarli control diet

Research Diet #L10016 – Lieber-DeCarli ethanol diet

Teklad extruded rodent diet – Breeder's chow

Table 2.2 Antibodies used for immunoblot and immunofluorescent analysis

Antibody	Dilution	Application	Source
β-Actin	**1/500**	**IB**	Santa Cruz Biotechnologies, Santa Cruz, CA
Amylase	**1/1000**	**IB**	Calbiochem, San Diego, CA
ATF3	**1/500**	**IB**	Santa Cruz Biotechnologies, Santa Cruz, CA
ATF4	**1/500**	**IB**	Santa Cruz Biotechnologies, Santa Cruz, CA
ATF6	**1/500**	**IB**	Santa Cruz Biotechnologies, Santa Cruz, CA
CD4	**1/500**	**IF**	BD Pharmingen, Mississauga, ON
CPA	**1/1000**	**IB**	Cedarlane Laboratories, Hornby, ON
BiP	**1/1000**	**IB**	Cell Signalling Technology, Pickering, ON
eIF2α	**1/500**	**IB**	Santa Cruz Biotechnologies, Santa Cruz, CA
GADD34	**1/500**	**IB**	Santa Cruz Biotechnologies, Santa Cruz, CA
LC3I/III	**1/500**	**IB, IF**	Cell Signalling Technology, Pickering, ON
pPERK	**1/500**	**IB**	Cell Signalling Technology, Pickering, ON
peIF2α	**1/500**	**IB**	Cell Signalling Technology, Pickering, ON
XBP1	**1/500**	**IB**	Santa Cruz Biotechnologies,Santa Cruz,CA

IB = immunoblotting; IF = immunofluorescence